Title
Profiling antibody immune markers using nucleic acid systems

Author
Tsai, Cheng-ting

Publication Date
2018

Peer reviewed|Thesis/dissertation

Profiling Antibody Immune Markers using Nucleic Acid Systems

By

Cheng-ting Tsai

A dissertation submitted in partial satisfaction of the
requirements for the degree of

Doctor of Philosophy

In

Chemistry

in the

Graduate Division

of the

University of California, Berkeley

Committee in charge:
Professor Carolyn R Bertozzi, Co-chair
Professor David E. Wemmer, Co-chair
Professor Ming C. Hammond
Professor Seung-Wuk Lee

Spring 2018

Profiling Antibody Immune Markers using Nucleic Acid Systems

By
Cheng-ting Tsai
Doctor of Philosophy in Chemistry
University of California, Berkeley
Professor Carolyn Bertozzi, Co-chair
Professor David Wemmer, Co-chair

Technology to profile nucleic acid materials has been greatly advanced over the past decade. Nowadays, tools such as real-time quantitative PCR (qPCR) and next generation sequencing (NGS) are standard workhorses for biomedical laboratory. However, in contrast to great advance in nucleic acid science, assays used to quantify proteins and antibodies immune markers remain much stagnant. Traditional immunoassays such as enzyme linked immunosorbent assays (ELISA) and western blots, invented almost half a century ago, are still widely used. These assays face limitations including low sensitivity, low specificity, limited multiplex power and requirement of large sample volumes. To this end, I have thought to create a methodology that allows researchers to leverage advanced nucleic acid tools to profile protein and antibody immune markers. In this thesis, I will provide an overview on current landscapes of nucleic acid-based assays for protein immune markers, and discuss how the new nucleic acid-based assay that I developed differentiates and complements other nucleic acid tools. Then, I will describe in details about our new assays including the creation of protein-DNA conjugates and use of these reagents to transform protein/antibody identities into quantifiable nucleic acid signals. Furthermore, I will describe impact of such methods in research and clinical settings by two selective applications. Finally, I will discuss further development that is required to make this assay widely deployable in research and clinical communities.

Acknowledgement

First of all, I can't thank my parents enough to nourish me in a highly supportive environment, where I can freely explore things that interest me the most. Under their shelter, I could pursue my careers with little worries and concerns. I am sure I wouldn't be where I am without them, and thus I wish to credit all my success, if there is any, to them.

Secondly, I am still grateful today that I have the opportunity to join Carolyn's lab, given my odd background. Back at the day I joined Carolyn's lab, there were very few biophysical studies. And when Carolyn pitched the only few biophysical projects to me, I turned her down right way. Instead, I told her on the first day that I would want to do more translational research. Looking back, this was a quite unusual and bold request. Thankfully, just as my parents, Carolyn gives the full freedom to me that I can explore any topics that I want. Moreover, she has been supporting me in any way she can. Unlike a traditional PhD training, which are highly research focus, she gives me the chance to initiate numerous grant writing. She let me participate in numerous workshop and program to broaden my skill sets way beyond science. She grants me the full freedom to initiate countless collaborations and take the lead on those projects. All these things cumulatively enable me to become a much more rounded researcher. I believe I will always look up to Carolyn as a career role model. I wish I could be a fine scientist, mentor and entrepreneur one day, just like Carolyn is.

Thirdly, I also want to thank Peter, who I have been working with days and nights over the past 5 years. When I first joined the lab, Peter has the generosity to share his project with me and teach me the fundamental about biological research. The longer I stay in graduate school, the more I realize how kind and generous he has been. I also enjoy the old days we bounced idea off on the 8th floor at Latimer Hall. Wish we could continue the scientific pursuit for many years to come.

I also want to give a shout out to David. I have the fortune to know him over the past three years. I have learned so much from him, and it is a pleasure to have someone coming out from an entirely background to exchange perspective with. I am definitely grateful to have a colleague and friend like him.

Certainly, all the lab mates I have the fortune to work with over the past 5 years make my PhD journey a lot more colorful. I still remembered that Doug gave me a box of chocolate as Christmas gift back at 2013, which made my first ever Christmas away from hometown much warmer. I appreciate all the hospitality that I received. That really makes fitting into a new country, a new

lab and a new environment a lot more joyous.

Finally, I would like to thank my fiancée Yuchi for her company and support. There are many ups and downs in the past five years. With her, I feel I have the courage to face the challenges and embrace the results no matter good or bad.

Jason
2018 March 16th

Chapter 1
Overview of nucleic acid-based assays for proteins quantifications

Chapter 1. Overview of nucleic acid-based assays for protein quantifications.

Profiling nucleic acids materials has greatly transformed our understanding of biological processes. In the past decades, numerous nucleic acid characterization tools have been developed, including nucleic acids microarray (e.g. Affymetrix arrays), real time quantitative PCR (qPCR) and next generation sequencing (e.g. Illumina, Oxford Nanopores). These innovative technologies have disrupted the barriers in profiling nucleic acids in both research and clinical settings.

In contrast to the explosive advance of nucleic acid characterization tools, assays to study proteins and antibodies remain much stagnant. Nowadays, traditional western blots and enzyme-linked immunosorbent assays (ELISA) are still widely used, despite the fact that they are first developed more than 50 years ago. In this thesis, I seek to bring innovations made in the nucleic acid field to protein and antibodies characterizations, with a hope that a more sensitive, multiplex, robust and cost effective tool can be made available for wide research and clinical communities.

Nucleic acid based protein characterization tools

I am certainly not the first person to think about bringing advanced in nucleic acid characterization technology to protein fields. I will highlight briefly a few well-established assays in this thesis. They all share the common feature that they transform protein identities into nucleic acid barcodes. Yet they differ in methods to perform the transformation and downstream nucleic acid barcode characterization.

The first tool I would like to highlight is an assay system termed immuno-PCR. The first landmark paper describing immune-PCR is first published in Science back at 1992[1]. Immuno-PCR is probably the most straightforward method to transform identities of proteins to DNA barcodes. Briefly, the whole assay resembles an ELISA. But instead of using antibody-enzymes (e.g. antibody-horse peroxidase (HRP), antibody-phosphatase), one would use antibody-DNA conjugates as reporters. The idea is illustrated in **Figure 1A**. A first antibody is immobilized on the substrate, which can bind and pull down protein targets in the samples. Then, after washing off unbound substances in the sample, one would add in antibody-DNA conjugates. The conjugates would bind onto a different epitope on the protein target and retain on the substrates. Then again, one would wash off unbound antibody-DNA conjugates by

excessive washing step. Finally, one can extract the DNA and quantify by qPCR method. Methodology to extract the DNA includes proteinase treatment or employment of a cleavable linker between the antibody and DNA barcode. Indeed, this method improves over traditional ELISA in that it can leverage exponential amplification power of PCR on DNA to achieve highly sensitive detection of protein analytes. Despite the inspiring technical performance, the real-world application of immuno-PCR seems to be limited in very few applications. One of the major issues is assay specificity. Since DNA amplification is highly sensitive, even slight residual amount of non-specific antibody-DNA conjugates bound on the substrate would lead to detectable background signals. Thus, one has to develop very sophisticated washing condition in order to prevent such false positive signals from being generated. To the best of my knowledge, Chimera Biotec GmbH (German) is one of the very few active service providers for immuno-PCR assays. In addition, there is only one FDA approved immuno-PCR based assay, termed NADiA ProsVue for quantification of prostate specific antigen (PSA). The assay is fist marketed by Iris International, which is later acquired by Danaher. However, after the acquisition, I believe the assay is not widely available to the general patient population anymore, if available at all. Based on these facts, one would believe there is still room to be improved for immuno-PCR based assays to enhance its practicality.

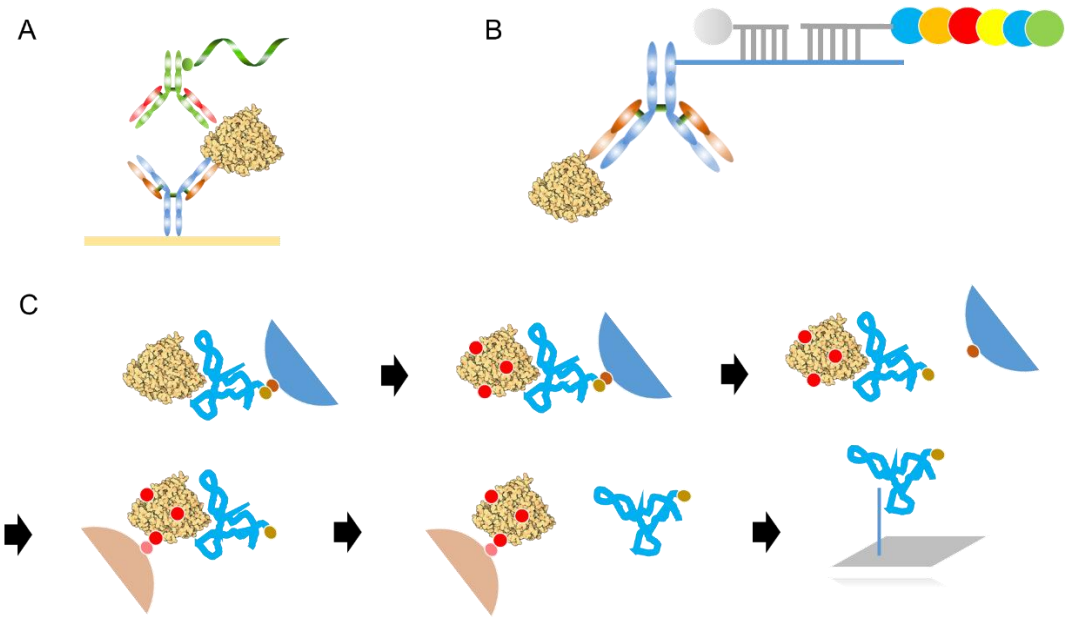

Figure 1. Principles for nucleic acid-based protein detection assays. A, Immuno-PCR B, Nanostring C, Somalogic's SOMAscan.

The next assay I would like to highlight is conceptually similar to immuno-PCR. The assay is termed Nanostring assays, which is first published at Nature Biotechnology back at 2008[2]. The assay resembles immuno-PCR in that it also uses nucleic acid tags as reporters. However, Nanostring does not require PCR amplification to achieve quantification. Instead, Nanostring uses its unique microfluidic microscopy system to visually count the numbers of nucleic acid tags, wherein the number of tag counts is directly proportional to the analyte concentration. To briefly explain the assay principle, please first take a look at Figure 1B. The nucleic acid tags are a few hundred based pairs of double stranded DNA that are color coded. The colors are appended by complementary binding between dye conjugated single-stranded DNA with the single stranded tag scaffold. The idea is that each tag has a unique color combination such that they are visually distinct under a microscope. However, one would argue if Nanostring simply uses color coded nucleic acid tags as reporters, the assay specificity will not and should not be any better than immuno-PCR. The likelihood of non-specific binding of Nanostring nucleic acid tags to the surface should be as bad as immuno-PCR conjugates. Although detailed reasons for Nanostring's high specificity has not been published, I presume there are two possible explanations. The first reason is that Nanostring (the company who are developing Nanostring technologies) licensed a very special surface treatment technology termed OptiChem Coating from Accelr8 Technology corporation. This special surface treatment method is first published in Chemistry Materials[3], wherein it describes the film to contain a mixture of four to five special chemicals (e.g., NHS-PEG-NHS, aminosilane and azidosilane, to name a few). Given that Nanostring pays significant royalties (over $200K) to Accler8 and has renewed the licensing agreements multiple times, I presume this special formulation has played a significant role in achieving outstanding specificity. In addition, Nanostring's assay requires strong buffer flow to fully extend their tags, such that the color codes will be more readable. The strong buffer flow may possess more effective washing capabilities than normal pipetting based washing step. Finally, just to help us put the specificity into context, in a typical Nanostring experiments, there are more than 10,000 reporter tags added into the assays. Surprisingly, the mean background tag count is typically 5-10 tags! Though it is not perfect (which will be 0 residual tag), Nanostring assay seems very close to perfection, in term of specificity. Indeed, Nanostring assays are FDA approved and actively being used by thousands of researchers and clinicians worldwide. It takes a lot of effort to get the assay specific, but I think it well pays off.

Thirdly, another highly successful nucleic acid based assays for protein quantifications are SOMAscan platform[4], developed by Somalogic (Boulder, Colorado). Though SOMAscan assays might look quite distinct from previous two assays, it still employs a reporter that contains an affinity tag and a DNA barcode. However, in this case, the affinity tag is also a piece of single-stranded DNAs. To those who are familiar with the matters, SOMAscan's affinity tag is called aptamer. Aptamer is a single stranded nucleic acid that is capable of binding specific analytes (just like antibodies). A natural question is why SOMAscan doesn't use antibody-DNA conjugates as reporters but use aptamers. The first reason is that despite both antibody and aptamer are both capable of binding target with specificity, their productions are quite distinct. Antibodies are typically produced by animals or recombinant cell lines, whereas aptamers can be readily synthesized by mature solid phase nucleic acid synthesis technology. This renders the cost of production dramatically different. In addition, one can easily add unnatural nucleic acid materials to the aptamer scaffold during synthetic process and generate unique affinity probes that are not otherwise attainable (of course, you can make antibody with unnatural amino acid, but for those who ever try this, this is not an easy tasks at all. In fact, very few laboratory have capabilities to achieve this). For these reasons, it seems SOMOscan aptamer is an ideal reagent in that the affinity tag and DNA barcodes are "conjugated" naturally together, which make the production a lot easier than antibody-DNA conjugates. However, if this is just it, then the fundamental non-specific binding proteins that troubles immuno-PCR has not been solved yet. Chances are the aptamer probes can still non-specifically trapped to substrate surfaces and generates background signals. In order to prevent this, SOMAscan built in two regulatory step, as shown in Figure 1C. Firsly, SOMAscan aptamers are anchored onto microsphere ("beads") with a photo-cleavable linker. Thus, if the SOMAscan aptamer are somehow trap onto the beads by some non-specific interactions, they will not be released from the beads even after photocleavage. Secondly, they use a biotin-NHS labeling to label all the protein and then pull down with streptavidin beads. Then, SOMAscan aptamers are eluted with detergent. The idea is that only aptamer with proteins bound on it will be pulled down, and thus eluted. These two checkpoints should help eliminate many non-specific binding event. However, these two checkpoints are certainly not yet perfect, one can still conceive many ways that non-specific binding proteins can evade these checkpoints. But as far as practical experience goes, Somalogic offers their SOMAscan as customer services, and are known for highly accurate and reproducible results.

Fourthly, Olink Biosciences have another assay system called Proximity Extension Asssays (PEA) where they make a pair of antibody-DNA conjugates as reporters[5]. However, they design their probes in a way such that they are not individually amplifiable. Their probes only become capable of signal generation after they are brought into close proximity by the protein analytes. It appears that this requirement for proximity has made their assays highly specific. Indeed, Olink has offer their PEA assays service for wide range of customers, and known for their high assay quality.

Lastly, there are many other nucleic acid characterization technology for proteins analytes that are beyond the scope of this thesis. For instance, one can view phage display library as a nucleic acid assays as well. In this special case, the nucleic acid barcodes are the inherent genomic materials inside the phages, and the "affinity probes" are the surface proteins expressed on the surface of the phages. The two components are thus naturally "conjugate" together. This method can achieve high content of multiplexing that is not possible by synthetic methods (e.g. aforementioned Nanostring, Somalogic and Olink assays are all restricted to analyze 100-1000 targets in a single assay, whereas phage display can easily go up to 10^5.)

Coexistence of nucleic acid characterization tools for protein analytes.

After reading about all these different tools, one might argue that why these technologies all exist despite their high similarity. And why wouldn't one technology just outcompete another technology and dominate the fields.

I have been pondering about this question for a very long time. I still don't know the answer to this. But I presume it is because each entities only have so "limited" resources and bandwidths, such that they can only work on limited things. If one take a look at Nanostring, they mostly focus on applying their technologies to gene profiling. They only recently added the protein quantifications capabilities to their product menu. Their products are mostly focus on gene and protein panels relevant to oncology. They only recently expand their panel for neurology, and is working on some other diseases. Even so, each of the panel only has 800 genes and 50-60 proteins. That being said, due to the "limited" resources, they have to consolidate their understanding about human biology and make their best guesses on what are the most common targets people would want to test for. In that sense, there are certainly scenario where interesting genes/proteins targets are not covered by their assays.

Similarly, Somalogic offers their SOMAscan that includes approximately

1000 common protein targets. Whereas O-link offers 13 different panels (e.g. oncology panel, cardiovascular panel, metabolism panel) and each panels cover approximately 90-100 protein targets. That being said, each assay developer makes their own unique guesses on what are the valuable targets people would want to look for. As long as their guesses are not entirely overlapping, they are mutually nonexclusive despite some similarity in the technologies.

Therefore, I also believe a successful technological platform is only the minimum criteria to success, but only if it is pair up with a correct applications will it come into fruition.

Format of deployment

As a scientist, we tend to focus more on the technical merits of the technology such as who are more sensitive, more multiplex and more specific. Yet as mentioned above, the correct application could be just as important as the technical performance. And depending on the applications, the way the assays are offered is also important.

For all aforementioned nucleic acid assays, only Nanostrings offers their assays and instruments as standalone products that researchers could purchase. On the contrary, Somalogic and O-link Biosciences only offer service to their assays but do not sold reagents kits and instruments. And indeed, none of the assays mentioned above are close to become a point of care (POC) assays, which could be deployed in a small clinic. (Nanostring's only diagnostics product Prosigna, which is a breast cancer prognosis tests, require a freezer size instruments that costs over $300K, which is no way possible affordable in a small clinic).

Thus, it appears that none of the nucleic acid based assays for protein analytes have overcome the technical hurdles that would render them applicable in POC settings. This is probably because POC based nucleic acid tests only become available in recent years (2005 and beyond). Thus, by the time those nucleic acid protein assays are developed, there are still no existing infrastructure on POC DNA test they can tap into. This also leaves an open space for those who are bold enough to make an effort in this regard.

To help briefly orient the readers on some of the POC DNA test available nowadays, I will highlight a few more mature technology. Fundamentally, all of the POC DNA test use microfluidic system to integrate nucleic acid extraction, amplification and quantification into a single system. The first platform is Cepheid POC PCR tests. The major features of Cepheid test is that they use

multiple color (Taqman assays) to achieve 3-6 plex in a single assay with turnaround time close to 70-100 min. The second platform is BioFire POC multiplex tests[6]. They use an array format in the final PCR quantification step to achieve quantification of 20-30 targets in a single assays with a turnaround time of 70 min. The third one is Rohce LIAT test, which is also a microfluidic based POC PCR tests that seems to be slightly faster than other options (~20-30 min from samples to results). The last one is Luminex's Verigene (previous Nanosphere, firs published in Science 2001) and Aries (acquired from GenturaDx). In the past 5 years, significant adoption of these technologies are seen in the clinical settings. I believe one day, one could integrate protein detection into these POC PCR platform to offer performance otherwise not achievable by traditional ELISA and western blots.

Position of this thesis in the context of nucleic acid tools.

During the PhD program, I have developed a series of technology to detect antibodies using nucleic acid characterization tools. As mentioned earlier, despite there are already many different nucleic acid tools for protein profiling, none of them have been applied to antibody quantifications. However, as the readers might know, antibodies on its own is a very important class of immune markers that have implications in essentially all human diseases. It is to my surprise that none of the nucleic acid protein assays ever been deployed for antibodies. In addition, antibodies quantifications faces unique challenges that are not seen for protein quantifications, in that some antibodies only bind onto conformational epitopes. Thus traditional solid phase assays format such as ELISA and western blot often failed. In addition, antibodies could have different classes (e.g. IgG, IgM, IgA, IgE and IgD). The capabilities to selectively detect a subset of them or all them could have different clinical impacts. Lastly, as a scientific questions, antibodies are traditionally thought to be generated at least two weeks after infection. It is not clear whether we only see antibodies after two weeks because current assays are not sensitive enough to pick it up earlier or our bodies simply won't generate (mature) antibodies before then. Therefore, the nucleic acid tool for antibodies quantification developed in this thesis should complement the current landscapes of nucleic acid tools. The development I made could potentially make quantification of DNA/RNA, protein and antibodies in a single platform possible.

Position of this thesis in the context of antibody quantifications.

I thought it is helpful to elude a little bit into how the antibody quantification

tool I developed sit in the antibody immunoassay field. Current antibody assays are still widely dominated by ELISA and western blots. However, as mentioned earlier, these assays on one hand failed to detect antibodies that only recognize conformational epitopes, and on the other hand lack the analytical sensitivity to detect trace amount of antibodies generated during the early phase of infection. Therefore, I foresee the antibody assays described in this thesis could help transform the use of antibody biomarkers in the clinical settings.

Summary of rest of the thesis.

In the following chapters, I will describe the technology behind the antibody assays that I developed. Then, I will present a few selected validation studies to demonstrate the utilities of the antibody assays. I hope you will enjoy reading this thesis.

REFERECNES

1. Sano T, Smith CL, Cantor CR. Immuno-PCR: very sensitive antigen detection by means of specific antibody-DNA conjugates. *Science* 258(5079):120-2 (1992).

2. Geiss, G.K., et al. Direct multiplexed measurement of gene expression with color-coded probe pairs. *Nat Biotechnol.* 26(3):317-25 (2008)

3. Harbers, G.M., et al. Functionalized poly(ethylene glycol)-based bioassay surface chemistry that facilitates bio-immobilization and inhibits nonspecific protein, bacterial, and mammalian cell adhesion. *Chem Mater.* 19, 4405 – 4414 (2007)

4. Gold, L., et al. Aptamer-based multiplexed proteomic technology for biomarker discovery. *PLoS One* 5(12):e15004 (2010)

5. Fredriksson S, Gullberg M, Jarvius J, Olsson C, Pietras K, Gústafsdóttir SM, Ostman A, Landegren U. Protein detection using proximity-dependent DNA ligation assays. *Nat Biotechnol* 20(5):473-7 (2002).

6. Poritz, M.A., et al. FilmArray, an automated nested multiplex PCR system for multi-pathogen detection: development and application to respiratory tract infection. *PLoS One* 6(10):e26047 (2011)

Chapter 2.
Development of antibody detection by agglutination-PCR (ADAP) technology.

Chapter 2. Development of antibody detection by agglutination-PCR (ADAP) technology*

In this chapter, I am going to describe the importance of antibody (or immunoglobulins) as biomarkers for diagnosis and prognosis of many pathological conditions. Moreover, I will highlight some of the challenges that frustrate current immunoassay analysis. With that background in mind, then I will describe approach and initial data on antibody detection by agglutination-PCR (ADAP) assays.

*Peter Robinson, PhD contributes significantly to results described in this chapter. The content of this chapter has been published at ACS Central Science, 2016.

Ultrasensitive antibody detection by agglutination-PCR (ADAP), ACS central science, 2016

INTRODUCTION

Circulating antibodies represent one of the most prevalent classes of biomarkers for human disorders including infectious[1], autoimmune[2], neurological[3], and oncological[4,5] diseases. Detection of low abundance antibodies using highly sensitive assays improves patient outcomes significantly by enabling early diagnosis and therapeutic intervention[4-6]. However, the physical deformation of antigen upon immobilization on solid supports impedes the detection of many disease specific antibodies by ELISAs, protein microarrays, lateral flow assays, or immuno-PCR[7-16]. Furthermore, the unpredictable orientation of surface-deposited antigen can conceal important epitopes for antibody binding[17].

Solution-phase approaches to antibody detection offer significant advantages. The solution-phase radioimmunoassay (RIA) is the current gold standard detection method for antibodies that only bind intact antigen[7], such as anti-insulin autoantibodies used for the early detection of type 1 diabetes[9,10]. RIAs are more sensitive than ELISAs but use hazardous radioactive reagents and demand laborious washing and centrifugation steps. Additionally, the limited multiplexing capacity of RIA hinders its application to the discovery of new antibody biomarkers. Consequently, current methods do not meet the need for an immunoassay that preserves the native conformation of antigens and enables sensitive, multiplexed detection of their cognate antibodies. Such a

method would greatly improve diagnostic strategies for diseases with conformation-sensitive antibody biomarkers and accelerate the discovery of underexplored biomarkers in various human pathologies.

We report the development of a new assay, antibody detection by agglutination-PCR (ADAP), for the robust and rapid detection of antibodies in asolution-phase format (**Fig. 1**). We took inspiration from two distinct assay formats: (1) the classic latex agglutination assay[19], where serum antibodies cluster antigen-latex particles into optically detectable complexes, and (2) proximity ligation assays in which protein-protein complexes are detected by PCR amplification. ADAP instead harnesses the agglutination power of antibodies to aggregate antigen-DNA conjugates to drive ligation of oligonucleotides and produce an amplifiable PCR amplicon (**Fig. 1**). The ligation event converts the PCR-incompetent half-amplicons on each antigen-DNA conjugate into a new and distinct PCR reporter[20]. Notably, this solution-phase step preserves the antigen's native conformation and eliminates the need for washing and centrifugation protocols to remove unbound secondary reporters[20]. These features significantly improved sensitivity over existing techniques while only requiring slight modifications to a standard PCR protocol.

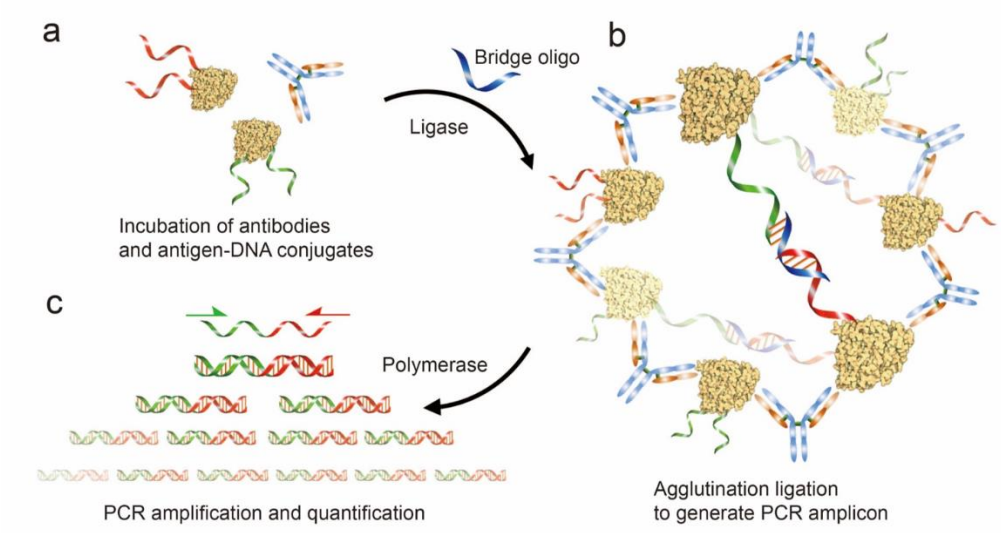

Figure 1. Schematic representation of antibody detection by agglutination-PCR (ADAP). (**a**) The sample containing the target antibody analyte is incubated with a pair of antigen-DNA conjugates. Each conjugate bears an oligonucleotide sequence comprising either the 5'-(red) or 3'-(green) half of a full amplicon. (**b**) Next, antibodies within the sample agglutinate the antigen-DNA conjugates and position them for ligation upon the addition of a bridging oligonucleotide (blue) and DNA ligase. (**c**) The newly generated amplicon (red/green) is exponentially

amplified with primers that bind their respective sites (red and green arrows) and quantified by real-time qPCR. The immune complex of antibodies and antigen-DNA conjugates shown here represents the proposed mechanism for detecting polyclonal antibodies with relatively large antigens at high concentrations. For monoclonal and anti-small molecule antibody detection, as well as when antibody concentration is significantly lower than that of antigen-DNA conjugates, the complex likely consists of a single antibody bound to two antigen-DNA conjugates (**Figure S5**).

RESULTS

Synthesis of antigen-DNA conjugates

Central to a sensitive ADAP assay is the creation of antigen-DNA conjugates. For protein antigens, we synthesized these components by lysine-to-thiol crosslinking using sulfo-SMCC and thiolated oligonucleotides[21]. Briefly, maleimides are installed on lysines of purified antigen by reaction with sulfo-SMCC in PBS. Thiolated oligonucleotides are activated by DTT-mediated reduction. Both antigen and oligonucleotides are desalted, pooled, and allowed to react overnight. Unreacted reagents are removed by extensive purification with size-exclusion spin columns. Antigen-DNA conjugation ratios are characterized by UV-Vis spectroscopy and observing a mass shift in PAGE (**Supplementary Fig. 1**). Typically, a 1:2 antigen-to-DNA conjugation ratio yields the optimal signal in ADAP assay. Overconjugating DNA to antigens can mask epitopes for antibody binding and thus lead to reduced assay sensitivity (**Supplementary Fig. 11**).

For small molecule antigens, succinimidyl ester-activated small molecules were incubated with amine-modified oligonucleotides in a one-step conjugation (Supplementrary Fig. 5a). The resulting small molecule DNA conjugates were characterized by high resolution mass spectrometry. Small molecules, in contrast to protein antigens, contain far fewer antibody epitopes. It is thus critical to design conjugation sites that still preserve the accessibility of epitopes to antibodies. In the case of dinitrophenol (DNP) antigens (**Fig. 4a** and **Supplementary Fig. 5)**, we choose the conjugation site to be identical to the one used to generate the DNP-BSA conjugate, which is the immunogen for the antibody we tested[33].

Workflow of antibody detection by agglutination-PCR (ADAP)

In a typical ADAP-based antibody detection experiment (Fig. 1), pairs of antigen-DNA conjugates are diluted in buffer. One antigen-DNA conjugate bears the 5’ half of a PCR amplicon while the other conjugate bears the 3’ half

that is 5' phosphorylated to enable ligation. The pooled conjugates are added to 2 µL of antibody-containing analyte and incubated for 30 min to allow binding. Next, DNA ligase and a bridging oligonucleotide are added and incubated for 15 minutes. Following selective hydrolysis of the bridging oligonucleotide, the ligation mixture is pre-amplified and the resulting products are analyzed by qPCR. Importantly, high Ct values of qPCR are associated with low assay reproducibility[35]. The inclusion of a pre-amplification step in ADAP helps maintain the Ct value for both samples and blank controls within the range of 10-20 and thus yields low intra-assay (<1%) and inter-assay (<3%) variations[35].

In vitro validation and specificity/sensitivity analysis

As a first target, we synthesized insulin-DNA conjugates to detect anti-insulin antibodies. Insulin autoantibodies are an important early biomarker of type 1 diabetes[9], but the development of a standard immunoassay is thought to be frustrated by the denaturation of insulin on solid supports[10, 22]. Currently, a radioimmunoassay is the principal technology for detecting insulin autoantibodies[10, 22]. A solution-phase PCR assay would reduce the amount of time needed for the test and remove the requirement of radioactive reagents.

We serially diluted affinity-purified anti-insulin antibodies into various biological matrices and analyzed them by ADAP. We observed a dose-dependent response across five orders of magnitude with very similar results obtained in different biological diluents (**Fig. 2a).** The detection limit in serum was found to be 170 zeptomoles of antibody in a 2 µL sample (**Supplementary Table 1**). We performed a head-to-head comparison with a direct ELISA and found an 865-fold improvement in limit of detection (**Fig. 2b** and **Supplementary Table 1**). The specificity of ADAP was determined by assaying samples containing isotype control antibodies, which yielded no detectable signal (**Fig. 2c**). Similarly, no detectable signal was observed when the assay was performed with irrelevant antigen-DNA conjugates (Supplementary Fig. 12). These results demonstrate that ADAP detects target antibodies with superior sensitivity and specificity over traditional methods while only using much smaller volume of material.

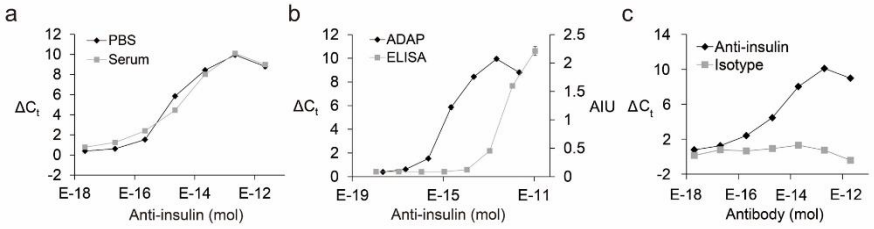

Figure 2. Sensitivity and specificity of ADAP. (a) Detection of serially diluted purified anti-insulin antibodies in phosphate buffered saline (PBS) or bovine serum. The x-axis displays the moles of antibody in a 2 μL sample. The y-axis is △Ct calculated by the difference of Ct value between the sample and a blank. (b) Head-to-head comparison with an ELISA for the detection of anti-insulin antibody. The right y-axis represents arbitrary intensity units (AIU) from the ELISA. (c) The specificity of ADAP was investigated by analysis of serially diluted isotype IgG in serum. No detectable signal was observed. Error bars represent standard deviation from triplicate samples, but for many data points are too small to be visualized.

To show that ADAP scales over a broad range of antigen molecular weights, we assayed antigen-antibody pairs for biotin (~0.24 kD), GFP (26 kD) and mouse-IgG (150 kD). For all three pairs, ADAP consistently detected low attomoles of antibody (**Fig. 3**, **Supplementary Table 1** and **Supplementary Fig. 2-4**).

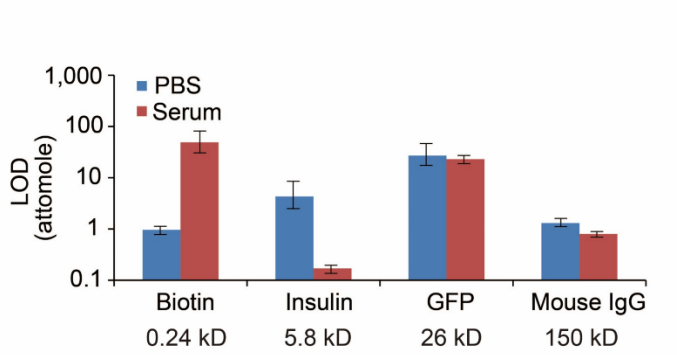

Figure 3. ADAP detects zeptomoles to attomoles of antibodies that bind antigens across a wide molecular weight distribution. The limits of ADAP detection for anti-biotin, anti-insulin, anti-GFP, and anti-mouse IgG antibodies (antigen molecular weights of 0.24, 5.8, 27, and 150 kD respectively) was determined by analyzing antibodies added into PBS or bovine serum. Error bars represent the standard deviation from triplicate samples.

Detection of serum-derived antibodies against small molecules

Antibodies against small molecules can mediate allergic responses to drugs particularly those capable of covalently modifying host proteins[23]. However, the detection of small molecule binding antibodies by solid-phase immunoassay is challenging. Small molecules do not adsorb readily to plastics used in common immunoassays and therefore require specialized surfaces to produce an appropriate substrate[24]. We were curious whether anti-small

molecule antibodies could be detected by ADAP given that the presumably limited ability of such conjugate to form large aggregates (Supplementary Fig. 5b). As a model system, we synthesized dinitrophenyl (DNP)-DNA conjugates and incubated them with rabbit antisera from animals inoculated with DNP-BSA. Significantly, agglutination was detected with as little as 0.74 ng of total antiserum proteins (**Fig. 4a** and **Supplementary Fig.5** and **Supplementary Table 1**). This experiment demonstrates that ADAP can sensitively detect natively produced antibodies from whole serum and has the potential to monitor allergic responses to small molecules.

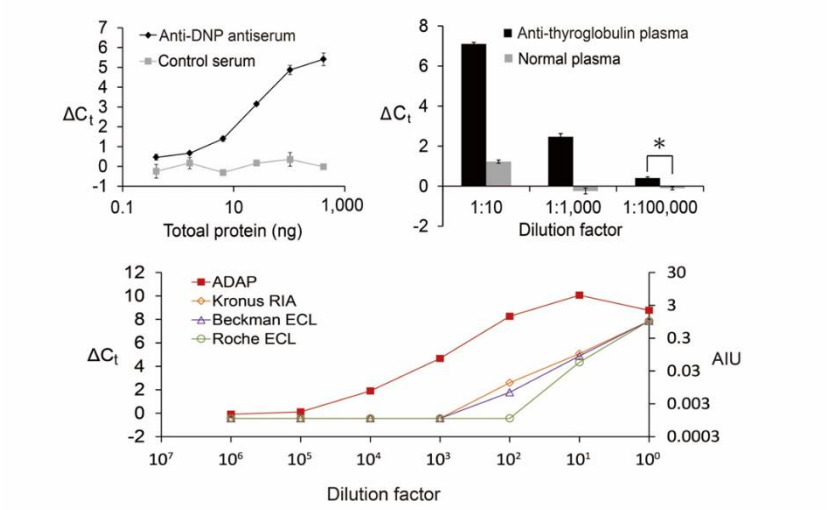

Figure 4. Detection of antibodies in mouse serum or human patient plasma and comparison with commercial diagnostics. (a) Detection of anti-dinitrophenol (DNP) from rabbit antiserum. Antiserum was serially diluted into PBS and analyzed by ADAP. A dilution series of antigen-naïve serum was analyzed as a negative control. (b) Detection of conformation sensitive anti-thyroglobulin from patient plasma. Anti-thyroglobulin-positive patient plasma was diluted into PBS as indicated and analyzed by ADAP. Anti-thyroglobulin-negative plasma from healthy subjects was analyzed as a negative control. (*P<0.01) (c) Identical samples of anti-thyroglobulin-positive human plasma were analyzed by ADAP, an FDA-approved radioimmunoassay (Kronus RIA) and two electrochemiluminescent assays (Beckman and Roche ECL).

ADAP is 1000 fold more sensitive than clinically used techniques

Next, we used ADAP to detect antibodies directly from patient samples. Thyroglobulin autoantibodies mediate and are diagnostic of autoimmune thyroiditis[25]. They can also be a critical biomarker for monitoring thyroid cancer

recurrence following therapeutic thyroidectomy[12]. A widely applicable, sensitive, and accurate detection assay for anti-thyroglobulin autoantibodies could prevent misdiagnosis of cancer recurrence and prevent unnecessary treament for healthy patients[12]. Currently, radioimmunoassays remain the gold standard for detecting this autoantibody[12]. However, only specialized laboratories retain the full capacity to perform this test, as stringent regulations for use and disposal of radioactive reagents limit widespread adoption. We hypothesized a PCR-based ADAP assay would preserve or improve upon the functional properties of a radioimmunoassay for detection of anti-thyroglobluin autoantibodies while obviating the need for radioactive components. We analyzed anti-thyroglobulin-positive patient plasma in an ADAP assay with thyroglobulin-DNA conjugates, and used healthy human plasma as a negative control. Agglutination was observed from the anti-thyroglobulin-positive samples (2 µL) down to 10^5-fold dilution with nearly no background from the healthy sample (**Fig. 4b**). Identical dilution series from both plasma samples were assayed using three FDA-approved clinical laboratory assays: radioimmunoassay (Kronus/ RSR), electrochemiluminescence assay (Beckman Coulter and Roche). Impressively, ADAP detected antibody binding with a detection limit 3-4 orders of magnitude lower than these standard assays (**Fig. 4c**).

Circumventing interference from anti-DNA autoantibodies

One potential confounding issue for ADAP is the interference from endogenous anti-DNA autoantibodies. These antibodies might agglutinate antigen-DNA conjugates in an antigen-agnostic manner and result in false positives. Patients suffering from autoimmune disorders such as systemic lupus erythematosus (SLE) often produce anti-DNA antibodies in high titer[26]. They are also generally present in small quantities in about 10 percent of healthy adults[27]. We obtained patient plasma that was independently verified to harbor anti-DNA antibodies and normal plasma with much lower levels of anti-DNA antibodies as a negative control. We used GFP-DNA conjugates as a neutral antigen to observe the extent of interference from anti-DNA autoantibodies, since there should be no naturally-occurring anti-GFP antibodies in human plasma.

As expected, we observed strong signal from anti-DNA-positive patient plasma and weak yet robust signal from normal plasma (**Fig. 5a**), demonstrating that these antibodies can interfere with ADAP analysis. Interestingly, after spiking in anti-GFP antibodies, identical dose-response

curves were observed for both anti-DNA-positive patient plasma and normal plasma (**Supplementary Fig. 6**). This observation is consistent with the notion that high affinity anti-GFP antibodies dominate the agglutination event and ADAP signal regardless of the presence of anti-DNA antibodies.

In an abundance of caution, we sought a general solution to circumvent potential interference from anti-DNA autoantibodies. To this end, we titrated in free DNA as a competitor to “protect” the antigen-DNA conjugates from counterfeit aggregation (**Fig. 5b**). At 100 μM of the competitor DNA, we no longer observed spurious signal from anti-DNA antibodies (**Fig 5b and Fig. 5c**). To validate that competitor DNA does not otherwise complicate ADAP performance, both anti-GFP antibodies and competitor DNA were spiked into anti-DNA positive plasma and normal plasma (**Fig. 5d**). ADAP analysis of these samples showed the expected dose response with no interference from anti-DNA antibodies. The limit of detection of anti-GFP antibodies in human plasma was similar tothat in buffer (48 and 27 attomoles respectively). Together, these results demonstrate that the addition of competitor DNA allows us to circumvent interference in human plasma samples.

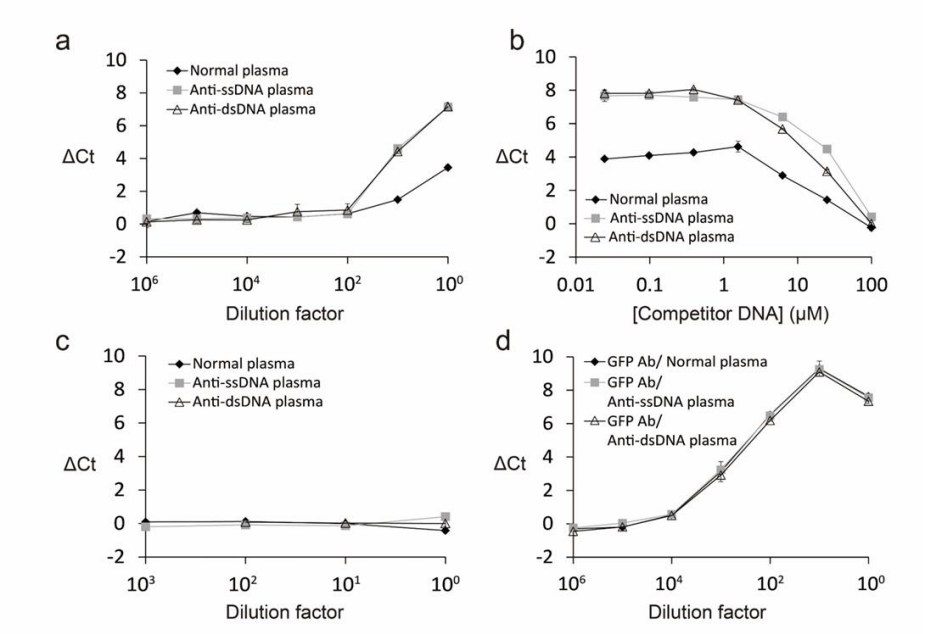

Figure 5. Circumventing interference from anti-DNA autoantibodies by competition with free DNA. (a) Investigation of interference from anti-DNA autoantibodies. GFP-DNA conjugates were used to analyze anti-DNA-positive patient plasma and healthy normal plasma. Patient samples were grouped into those containing anti-single-stranded DNA antibodies (ssDNA) and those with anti-dsDNA antibodies (dsDNA). Interference was observed at dilution factors

of 1 and 10 for all sample types (b) Competitor DNA was titrated into undiluted patient and normal plasma. The addition of competitor DNA eliminated background signal from interfering antibodies. (c) The experiment in (a) was repeated but with the addition of 100 μM competitor DNA which eliminated interference. (d) Purified GFP antibodies were added to anti-DNA positive and normal plasma. Detection of GFP antibodies was performed in the presence of 100 μM competitor DNA in all samples to confirm that it did not disrupt ADAP performance.

Multiplexed detection of antibodies by DNA barcoding

Multiplexed detection of several antibodies can be accomplished by use of orthogonal DNA sequence pairs to barcode distinct antigens. Diseases such as type 1 diabetes have multiple autoantibody biomarkers[9] (anti-Insulin, anti-IA-2, anti-GAD, anti-ZnT8) and several clinical protocols use antibody panels to establish a diagnosis. A barcoded assay could help in this regard by detecting antibodies in a single test.

We generated a set of orthogonal antigen-DNA conjugates with either biotin (Sequence Set 1; **Supplementary Table 2**) or mouse IgG (Sequence Set 2; **Supplementary Table 2**) as the antigen. The amplicons were designed such that Set 1 primers did not amplify the Set 2 amplicon and vice versa. The two sets of antigen-DNA conjugates were pooled and incubated with anti-biotin, anti-IgG antibodies, or both and then analyzed by ADAP. The sample incubated with the anti-biotin antibodies showed signal only with Set 1 primers, while the sample incubated with the anti-mouse IgG antibodies showed signal only in the Set 2 primers. The mixed sample containing both antibodies generated signal with both sets of primers (**Fig. 6a** and **Supplementary Fig. 7**). Importantly, there was no detectable cross-talk in this multiplexed experiment.

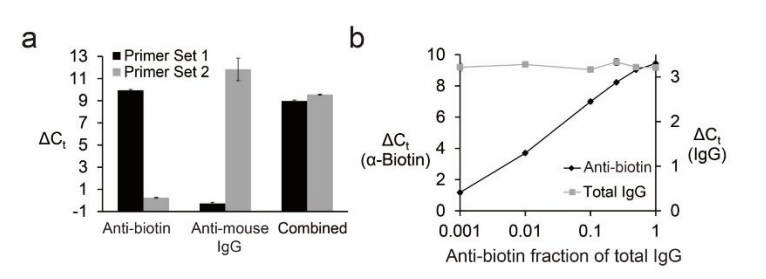

Figure 6. ADAP can be multiplexed. (a) Detection of two orthogonal antibodies in one ADAP experiment. Biotin-DNA and mouse IgG-DNA conjugates bearing either DNA sequence 1 or 2 (Table S2), respectively, were incubated with either anti-biotin antibody only, anti-mouse IgG antibody only, or both antibodies

together, and then analyzed by ADAP. (b) Multiplexed detection of anti-antigen antibody and total antibody levels by ADAP and proximity ligation assay (PLA), respectively. Biotin-DNA conjugates and anti-IgG-DNA conjugates were incubated with samples containing constant total IgG but varied fractions of anti-biotin antibodies. These samples were analyzed by ADAP and PLA. Error bars represent the standard deviation from triplicate samples, but for many data points are too small to be visualized.

Additionally, typical antibody tests do not take into account total immunoglobulin concentration. This can lead to false negatives for patients with immunoglobulin deficiency, which is a common problem in Celiac disease[28]. We envisioned that simultaneous detection of antigen-binding capacity and total immunoglobulin content could differentiate false negatives from abnormally low immunoglobulin levels.

To multiplex the detection of total IgG and antigen-binding ability, we generated anti-IgG proximity probes from a single batch of anti-IgG polyclonal antibodies. The batch was split into two pools and each was modified with either the upstream or downstream fragment of the Set 2 PCR amplicon. As in proximity ligation[20], the two halves are brought close together when the polyclonal antibodies bind nearby epitopes, allowing for ligation and subsequent detection by PCR. Goat anti-biotin antibodies were diluted into total goat IgG such that the total amount of IgG remained constant, but the anti-biotin fraction varied. ADAP analysis with the Set 2 primers showed no change in signal, corresponding to the constant concentration of IgG in every sample, whereas signal generated from the Set 1 primers increased as the fraction of anti-biotin antibodies increased (**Fig. 6b** and **Supplementary Fig. 8-9**).

Effect of antibody valency and clonality on ADAP performance

Finally, we wished to investigate the impact of antibody valency and clonality on the performance of ADAP. Serum antibodies are multivalent and polyclonal to allow optimal agglutination of pathogens for effective neutralization and clearance[29]. However, the limited agglutination power of Fab fragment and monoclonal antibodies[29] might preclude them from ADAP-based detection.

We incubated mouse IgG-DNA conjugates with either bivalent anti-mouse IgG or the corresponding monovalent fab fragment and analyzed them by ADAP. We expect no signal for the fab sample since fab fragments are monovalent and unable to agglutinate the antigen-DNA conjugates. Indeed, robust signal was detected for the anti-mouse IgG positive control and no

signals for fab fragment (**Fig. 7a**). Next, we incubated either polyclonal or monoclonal anti-GFP antibodies with GFP-DNA conjugates. Interestingly, both antibodies displayed similar limits of detection (**Fig. 7b**), but with very different dynamic ranges (about 6 or 4 orders of magnitudes for polyclonal or monoclonal antibody, respectively). We hypothesized that this difference was due to the saturation of binding sites when the concentration of the antigen-DNA conjugates matches that of the antibody analytes (the "hook effect"[30]). While the monoclonal antibody shows classic hook behavior when the antibody concentration (1.3 nM) is close to the antigen-DNA conjugate concentration (0.5 nM), the polyclonal antibody hook effect is delayed until a much higher antibody concentration (64 nM). We attribute this delayed hook effect to the availability of multiple antigen binding sites with polyclonal antibody. Polyclonal antibodies enjoy a higher effective epitope concentration and thus a wider dynamic range. These results demonstrate ADAP is well-suited for the detection of both poly- and monoclonal antibodies.

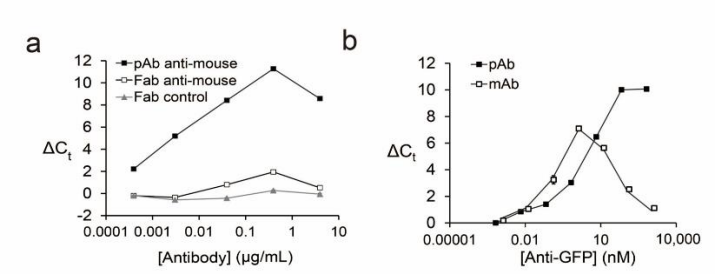

Figure 7. Effects of valency and clonality of the target antibody on ADAP performance. (a) Mouse IgG-DNA conjugates were incubated either with polyclonal anti-mouse IgG antibodies, monovalent Fab fragment anti-mouse IgG antibodies, or a control Fab fragment that recognizes unrelated antigens, and analyzed by ADAP. (b) GFP-DNA conjugates are incubated either with polyclonal or monoclonal anti-GFP antibodies and analyzed by ADAP. Error bars represent the standard deviation from triplicate samples, but for many data points are too small to be visualized.

DISCUSSION

We have developed an ultrasensitive multiplexable assay that uses PCR to detect antibodies from small volume samples A While it is true that many applications of proximity ligation have been realized over the past decade, they share the common format of using DNA-conjugated antibodies to detect an analyte of interest. Apparently it did not occur to practitioners of this technique that the assay could be wielded in perhaps its most powerful implementation by

inverting the scenario, wherein a DNA-conjugated analyte could be used for sensitive detection of antibodies. Of all the protein types one might want to detect in a clinical setting, antibodies are by far the most numerous. They are used as biomarkers of autoimmune diseases, cancers, infectious diseases, neurological disorders, and vaccine efficacy. Despite their high value as clinical diagnostic targets, there remain severe deficits in antibody detection assay development. The ADAP technology uniquely addresses the limitations of more conventional solid-phase ELISA-type antibody detection assays, and also possesses other elements of novelty that we believe distinguish this platform from other proximity ligation systems. As well, we believe that the mechanism by which the assay functions represents a significant departure from classic proximity ligation assays. We use the intrinsic bivalency of antibodies to drive the proximity effect, which has never been explored in the published literature to our knowledge. Furthermore, agglutination of the target antigen is a property unique to antibodies that is not observed with other protein classes already served by traditional proximity ligation assays. We believe that the impressive dynamic range observed from ADAP is directly linked to this unique property of antibodies. Supporting this argument is our data comparing the properties of poly- versus mono-clonal antibodies (**Fig. 7b**). The agglutination propensity of polyclonal antibodies leads to greatly improved dynamic range over a comparable monoclonal antibody. This mechanism is unique to antibody detection and to ADAP.

The advantages of the ADAP platform for antibody detection are considerable. As a solution phase assay, ADAP circumvents the protein denaturation and epitope masking problems of surface-immobilized-antigen based formats. While solution-phase assays such as the radioimmunoassay exist, they are difficult to perform, slow and have limited capacity for multiplexing. ADAP is 3 orders of magnitude more sensitive than clinically used assays, creating new possibilities for the early detection and treatment of disease. As a no-wash assay, ADAP eliminates the tedious optimization of washing and centrifugation steps that is necessary to minimize the loss of low-affinity antibodies. It does not require isolation of unique monoclonal antibodies as required for certain types of ELISAs. Since the ADAP does not rely on animal antibodies as capture reagents, it obviates interference from patient heterophilic antibodies[31].

The reduction in sample consumption and multiplexing capability lessen the demand for patient serum to promote patient compliance in applications requiring repeated monitoring. Significantly, ADAP is readily deployable in

many clinical settings, as it uses only conventional PCR equipment and reagents, which are standard devices in diagnostic laboratories. The custom reagents (antigen-DNA conjugates, ligation enzymes, and a bridging oligonucleotide) are used in ultralow quantities. For example, 100 µg of a 60 kDa antigen-DNA conjugate is sufficient to perform approximately ~1.7 million assays.

Infectious diseases such as HIV increasingly rely on combined antibody and antigen tests to improve confidence in diagnosis[32]. Combined with traditional proximity ligation[20] and PCR tests, ADAP opens the possibility of performing all three types of tests (nucleic acids, antigens, and antibodies) in a unified platform. ADAP could also be easily adapted to any number of novel point-of-care PCR platforms to provide highly sensitive solution phase antibody tests in low resource settings. Due to these favorable attributes, its operational simplicity, and the leveraging of existing technology, we predict that ADAP will provide a useful analytical platform for a multitude of clinical and research applications.

METHODS

Synthesis of antigen-DNA conjugates

Insulin-DNA conjugate was synthesized by resuspending recombinant insulin (Sigma-Aldrich) to make a 1 mg/mL solution in reaction buffer (55 mM sodium phosphate, 150 mM sodium chloride, 20 mM EDTA, pH 7.2). 1 µL of a 4 mM solution of sulfo-SMCC (Pierce Biotechnologies) in anhydrous DMSO was added to 10 µL of the protein solution and incubated at RT for 2 h. Thiolated-DNA (IDT) was resuspended to 100 µM in reaction buffer. 3 µL of the 100 µM thiolated-DNA stock was then added to 50 µL of reaction buffer. To this solution, 4 µL of a 100 mM solution of DTT (Life Technologies) was added to reduce the oxidized thiolated-DNA. The solution was then incubated at 37 °C for 1 h. 7k MWCO gel microspin columns (Life Technologies) were equilibrated with reaction buffer. The reduced oligonucleotides were desalted by the equilibrated microspin columns twice. Unreacted sulfo-SMCC was removed from the insulin solution by a 3k MWCO centrifugal filter column (EMD Millipore) to a final volume of 60 µL. The thiolated-DNA and insulin solutions were then mixed , reacted overnight at 4 °C and then purified by 10k MWCO filter column. Conjugate concentrations were determined by BCA assay (Life Technologies). Conjugation efficiencies were analyzed by SDS-PAGE and silver staining as described previously[37]. A representative silver-stain is shown in supplementary Fig. 10. DNA-to-antigen ration of the conjugates were estimated by UV-VIS

absorption. Antigen-DNA conjugates were stored at 4 °C for short-term usage or aliquoted for long-term storage at -80 °C. GFP-, mouse-IgG- and thyroglobulin-DNA conjugates were synthesized similarly with slight modifications. Briefly, unreacted SMCC was filtered by 7K MWCO gel microspin columns. Conjugates were purified from unconjugated DNA by centrifugal filter columns (GFP, 30k MWCO column; Mouse IgG, 100k MWCO column; Thyroglobulin, 100k MWCO column).

Finally, biotin-DNA conjugates were purchased from IDT. DNP-DNA conjugates were synthesized as follows. 25 mg DNP-NHS ester (Life Technologies) was dissolved in anhydrous DMSO to make a 50 mM solution. 5' or 3' amine functionalized DNA (IDT) was resuspended in ddH_2O to make a 1 mM solution. 40 µL of the 1 mM DNA solution was added to 300 µL of PBS with 50 mM $NaHCO_3$. 80 µL of the NHS ester solution was added over 2 d at RT under constant rotational mixing. Modified DNA was then precipitated by adding 2.5 volumes ethanol and 0.1 volumes 10 M ammonium acetate and then incubated for 4 h. Precipitated DNA was pelleted by centrifugation for 15 min at 4 °C, followed by a gentle wash in ice cold 70% ethanol-H_2O. The pellet was then resuspended in 100 µL ddH_2O and then purified again by precipitation as before to ensure complete removal of unreacted small molecules. After the second precipitation, the pellet was diluted in ddH_2O to make a 100 µM stock solution, which was stored at -20 °C until used. Synthesis was confirmed by high resolution LC-MS.

Antibody detection by agglutination-PCR (ADAP)

1 fmol of paired antigen-DNA conjugates were resuspended in 2 µL of incubation buffer C (2% BSA, 0.2% Triton X-100, 8 mM EDTA in PBS). 2 µL of analyte is added to the conjugates and then incubated at 37 °C for 30 min. 116 µL of ligation mix (20 mM Tris, 50 mM KCl, 20 mM $MgCl_2$, 20 mM DTT, 25 µM NAD, 0.025 U/µl ligase, 100 nM bridge oligo, 0.01% BSA, pH=7.5) was added, and then incubated at 30 °C for 15 min. 10 µL uracil-excision mix (0.025 U/µl Epicentre Bio) was added and incubated for 15 min at 30 °C. 25 µL of the solution was added to 25 µL 2x PCR Master Mix (Qiagen) with 10 nM primers and then amplified by PCR (95 °C for 10 min, 95 °C for 15s, 60 °C for 30s 12 cycles). The PCR reaction was then diluted 1:20 in ddH_2O. 8.5 µL of the diluted PCR samples were added to 10 µL 2x qPCR Master Mix (Life Technologies) with 1.5 µL primers (final concentration 690 nM). qPCR was performed on either a Bio-Rad CFX96 or a Bio-Rad iQ5 real-time PCR detection system.

The ADAP assays for affinity purified anti-insulin (Abcam), anti—biotin (Abcam), anti-GFP (Vector Laboratories) and anti-mouse IgG antibodies (Pierce Biotechnologies) were carried out as described above with the following modifications. For dilution in buffer, 2 μL of antigen-DNA conjugates were mixed with 2 μL of serial diluted antibodies (concentration range: 10^{2}-10^{-4} μg/ml) in buffer C or buffer only (blank). For dilution in fetal bovine serum (Sigma-Aldrich), antibodies were spiked in fetal bovine serum to obtain 2% (wt/wt) antibodies solution, which was then serial diluted in buffer C (concentration range: 10^{2}-10^{-4} μg/ml) for ADAP assay. For dilution in human saliva, human saliva was incubated at 95 °C for 15 min and centrifuged at 14000 g for 5 min to remove insoluble precipitates. Antibodies were spiked in processed human saliva at 1:1 volume ratio, which was then serially diluted in buffer C for ADAP assay. Isotype antibodies (Santa Cruz Biotech) subjected to the same preparation were analyzed side-by-side as negative controls.

ADAP detection assay for anti-DNP antibodies from antiserum.

The ADAP PCR detection assay for anti-DNP antiserum (Abcam) was carried out as described above with the following modifications. anti-DNP antiserum was obtained from rabbit inoculated with DNP-conjugated carrier proteins without further purification. 2 μL DNP-DNA conjugates were mixed with 2 μL of serial diluted anti-DNP antiserum (concentration range: 8-0.002 mg/ml) in buffer C for ADAP detection.

ADAP detection assay for anti-thyroglobulin patient plasma.

The ADAP detection assay for anti-thyroglobulin positive patient plasma (ImmunoVision) was carried out as described above with the following modifications. 2 μL Thyroglobulin-DNA conjugates were mixed with 2 μL of serially diluted patient plasma (dilution factor: 10^{0}-10^{6}) in buffer C for ADAP detection.

Multiplexed ADAP for anti-biotin and anti-mouse IgG antibodies.

Three sets of ADAP experiments were carried out to investigate the orthogonality of anti-biotin and anti-mouse IgG antibody detection. The multiplex ADAP assay for anti-biotin and anti-mouse IgG antibody was carried out as described above with the following modifications. 1 μL biotin-DNA conjugates (sequence 1 as in Supplementary Table I) and 1 μL Mouse-IgG-DNA conjugates (sequence 2 as in Supplementary Table I) are mixed with 2 μL of serial diluted either (1) anti-biotin antibodies (concentration range: 10^{2}-10^{-4}

μg/ml) in buffer C or buffer only (blank) (2) anti-mouse antibodies (concentration range: 10^{2}-10^{-4} μg/ml) in buffer C or buffer only (blank) (3) both anti-biotin and anti-mouse antibodies (concentration range: 10^{2}-10^{-4} μg/ml) in buffer C or buffer only (blank). The antigen and antibody mixtures were processed and analyzed as described above.

Multiplexed ADAP and PLA detection for anti-biotin antibodies and total IgG.

ADAP and PLA[20,21] (proximity ligation assay) were used in conjunction to quantify the specific antibodies and total antibodies amounts in a given sample. The multiplex ADAP detection assay for anti-biotin and total IgG was carried out as described above with the following modifications. 1 μL biotin-DNA conjugates (sequence 1) and 1 μL anti-Goat-IgG-DNA conjugates (sequence 2) are mixed with 2 μL of serially diluted either (1) goat anti-biotin antibodies (concentration range: 10^{2}-10^{-4} μg/ml) in buffer C or buffer only (blank) (2) goat IgG (concentration range: 10^{2}-10^{-4} μg/ml) in buffer C or buffer only (blank) (3) both anti-biotin and goat IgG in buffer C, where total IgG is fixed at 0.7μg/ml and anti-biotin antibodies fraction varied from 100%-0% or buffer only (blank). The antigen and antibody mixtures were processed and analyzed as described above.

Direct ELISA detection of anti-insulin antibodies.

Recombinant human insulin (Sigma) was resuspended to 1 mg/mL in PBS. 75 μL of the insulin solution was added to wells of an ELISA plate (Santa Cruz Biotech). The plate was covered with a plastic membrane and the insulin was allowed to adsorb to the plate overnight at 4 °C. Excess supernatant was decanted and the wells were blocked with 5% BSA in PBS overnight at 4 °C. Anti-insulin antibodies were diluted into PBS and allowed to bind at RT for 1 h. The supernatant was decanted and the wells were washed 4X with PBS. Secondary antibody-HRP probes (Santa Cruz Biotech) were diluted 1:5000 in 5% BSA in PBS and added to the wells and allowed to incubate at RT for 1 h. The supernatant was decanted and then washed 4X in PBS. 50 μL of TMB substrate solution as added and allowed to develop for 15 minutes and then quenched by addition of 50 μL of 2 M H_2SO_4. Absorbance was read at 450 nm in a plate reader.

Circumvent interference from anti-DNA antibodies.

Anti-DNA antibodies positive patient plasmas were purchased from

ImmunoVision. ADAP detection of anti-DNA plasma was carried out as described above with slight modifications. For detection of anti-GFP antibodies, anti-GFP antibodies are spiked into anti-DNA and normal plasma. A sample of 2 µL serial diluted anti-GFP solution is incubated with 2 µL solution containing GFP-DNA conjugates and with or without 100 µM competition DNA. The competition DNA is purchased from IDT with sequence below:
GGCCTCCTCCAATTAAAGAATCACGATGAGACTGGATGAA
TCACGGTAGCATAAGGTGCAGTACCCAAATAACGGTTCAC

Radioimmunoassay and electrochemiluminescent assays for anti-thyroglobulin autoantibodies

Tg-RIAs (Kronus), the Beckman Access TgAb (Beckman Coulter) and Roche Elecsys TgAb (Roche Diagnostics) were performed per the manufactures' instructions at University of Southern California. These assays are standardized against WHO reference serum 65/93. For assay details, see literature[38].

Data analysis

Three replicate ADAP measurements were carried out for each dilution of target antibodies in buffer C plus a blank. The replicates were measured by taking aliquots from the same dilution series and the same preparation of ligation, excision and pre-amplification steps but placing in three different wells in a PCR plate for qPCR analysis. Representative real-time PCR measurement plot taken from an ADAP assay for serial dilution of anti-biotin antibody was shown in **Supplementary Fig. 10**. A single threshold fluorescence value was automatically chosen by Bio-Rad software. For each curve, the PCR cycle number with fluorescence value corresponding to the chosen threshold value was defined as the cycle threshold (C_t) value. ΔC_t is defined as the C_t value of blank minus C_t value of samples[39]. The value of ΔC_t is proportional to the initial amplicon concentrations in the PCR plate well. This amplicon concentration is then also proportional to the amount of target antibodies present in the initial dilution series. A volume of 2 µL from each serial dilution series was taken for ADAP measurement. Thus, the number of antibody molecules in each measurement is (2×10^{-6} L) x Antibody concentration (M) x Avogadro's number. A non-linear four parameter logistic fit[40] for an antibody dilution series is determined using custom software. The limit of detection for the ADAP assay is defined as the average ΔC_t value of the buffer C only blank plus 3 standard deviation of the blank[41]. The value of limit of detection is calculated relative to

the blank.

Intra-assay and inter-assay variation for ADAP.

The intra-assay variation for ADPA was determined by repeating ADAP measurements in triplicate for anti-GFP antibodies six times on the same plate. The intra-assay variation is defined as standard deviation of the triplicate divided by mean of the triplicate[42] and is consistently <1%. The inter-assay variation for ADAP is evaluated by measuring anti-GFP antibody concentrations in triplicate on five different plates on different days. The inter-assay variation defined by standard deviation of concentrations from five different plates divided by mean of concentrations from five different plates[42] is <3%. Both the intra-assay and inter-assay variation of ADAP are far below the accepted biomedical assay variation values, which are 10% and 15% respectively[42]. ADAP's superior intra-assay and inter-assay performance is likely a result of having fewer overall handling steps, no wash steps, and no centrifugation steps. The extensive washing and centrifuging requirements for other assays might compromise their precision and reproducibility.

SUPPLEMENTARY MATERIALS

Antibody	Sequence	Diluent	Detection limit	
			ng/ml	*attomoles*
Anti-biotin	4	buffer	0.89 ±0.39	12 ±5
Anti-biotin	4	serum	3.7 ±2	49 ±27
Anti-biotin	1	buffer	0.072 ±0.008	0.96 ±0.11
Anti-Mouse IgG	4	buffer	1.9 ±0.6	25 ±8
Anti-Mouse IgG	4	serum	2.3 ±0.3	31 ±4
Anti-Mouse IgG	2	buffer	0.096 ±0.023	1.3 ±0.3
Anti-Mouse IgG	2	serum	0.060 ±0.008	0.8 ±0.1
Anti-GFP pAb	4	buffer	2.0 ±1.1	27 ±15
Anti-GFP pAb	4	Serum	1.7 ±0.6	23 ±8
Anti-GFP pAb	4	Human plasma	3.6±0.5	48±7
Anti-GFP mAb	4	Buffer	0.16 ±0.05	2.1 ±0.7
Anti-GFP mAb	4	cell culture media	0.12 ±0.05	1.6 ±0.7
Anti-Insulin	2	buffer	0.39 ±0.48	4.3 ±5.3
Anti-Insulin	ELISA	buffer	6.7 ±1.9	3722 ±1056
Anti-Insulin	2	serum	0.015 ±0.004	0.17 ±0.04
DNP	4	antisera	370 ±83	*N/A*

Table S1. Summary of limits of detection for various antibodies in different diluents and with different DNA sequences using ADAP. Antibodies were resuspended in the indicated diluent and then incubated with 2 µL of 0.5-1 nM

solution of the appropriate antigen-DNA conjugate. The limit of detection for the ADAP is defined as the average ΔCt value of the buffer C only blank plus 3 standard deviations of the blank41. The limit of detection is calculated relative to the blank.

Name	5' mod	Sequence	3' mod	Notes
Set 1A	thiol	CAGGTAGTAGTACGTCTGTTTC ACGATGAGACTGGATGAA	none	
Set 1B	phosphate	TCACGGTAGCATAAGGTGCAAG ATAATACTCTCGCAGCAC	thiol	
Set 1 bridge	none	CUACCGUGAUUCAUCCAG	none	Same as Set 2, U = deoxyribouracil
Set 1 F	none	GGCCTCCTCCAATTAAAGAA	none	Same as Set 2
Set 1 R	none	GTGAACCGTTATTTGGGTAC	none	Same as Set 2
Set 2A	thiol	GGCCTCCTCCAATTAAAGAATC ACGATGAGACTGGATGAA	none	
Set 2B	phosphate	TCACGGTAGCATAAGGTGCAGT ACCCAAATAACGGTTCAC	thiol	
Set 2 bridge	none	CUACCGUGAUUCAUCCAG	none	Same as Set 4, U = deoxyribouracil
Set 2 F	none	GGCCTCCTCCAATTAAAGAA	none	Same as Set 4
Set 2 R	none	GTGAACCGTTATTTGGGTAC	none	Same as Set 4
Set 4A	thiol	TCGTGGAACTATCTAGCGGTGT ACGTGAGTGGGCATGTAGCAAG AGG	none	
Set 4B	phosphate	GTCATCATTCGAATCGTACTGC AATCGGGTATTAGGCTAGTGAC TACTGGTT	thiol	
Set 4 bridge	none	GAAUGAUGACCCUCUUGCUA	none	U = deoxyribouracil
Set 4 F	none	CGTGGAACTATCTAGCGGTGTA	none	
Set 4 R	none	ACCCGATTGCAGTACGATTC	none	

Table S2. Oligonucleotide sequences19-22 used in ADAP. Set 1A, 1B, 2A, 2B, 4A and 4B represent the sequences for oligonucleotides on the antigen-DNA conjugates. Set 1F, 1R, 2F, 2R, 4F and 4R represent the primer sequences for qPCR quantification of the full length amplicons. Set 1 bridge, Set 2 bridge and Set 4 bridge represent the sequences for the bridge oligonucleotides as shown in Figure 1a.

Technology	ADAP	ELISA	RIA
Detection limit (attomole)	4.3	3722	32*
Sample volume	2 µl	100 µl	25 µl
# of assays 100 µg antigen	1.7 million	10-50	N/A
Assay time	< 3hr	< 4hr	3-24 hr
Multiplexability	2-50	<9	N
Solid support	N	Y	N
Washing/centrifugation	N	Y	Y
Radioisotope	N	N	Y
Detection device	PCR thermocycler	Plate reader	Gamma counter

Table S3. ADAP enjoys many advantages over common antibody detection methods. ADAP uses very low quantities of sample with ultralow reagent consumption in a solution-phase, wash-free, radioisotope-free assay. ADAP and ELISA values were calculated from in-house experiments, RIA from literature [Falorni, A.; Ortqvist, E.; Persson, B.; Lernmark, A. Radioimmunoassays for glutamic acid decarboxylase (GAD65) and GAD65 autoantibodies using 35S or 3H recombinant human ligands. J. Immunol. Meth. 1995, 186, 89-99.].

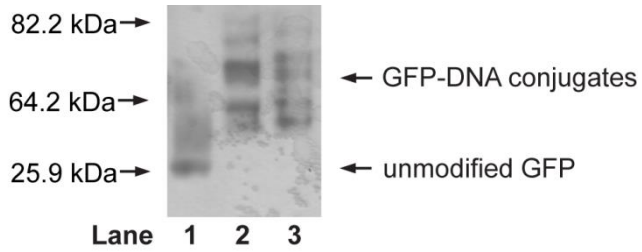

Figure S1. Representative silver stain of an antigen-DNA conjugate. Samples were resolved by SDS-PAGE and then total protein was visualized by silver staining. Lane 1 is unmodified GFP, lane 2 is GFP-2A conjugate and lane 3 is GFP-2B conjugate. A significant mass shift was observed in lanes 2 and 3 due to the addition a 14 kD oligonucleotide to the protein. Laddering of lanes 2 and 3 is a result of the addition of multiple oligonucleotides to a single protein.

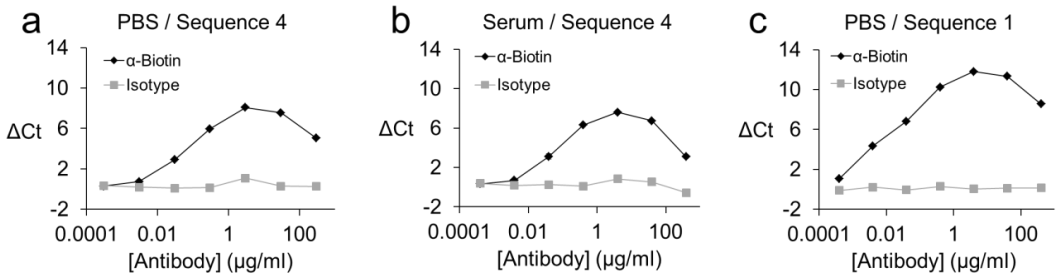

Figure S2. Representative ADAP curves from anti-biotin detection experiment. (a) Anti-biotin antibodies were incubated with biotin-DNA conjugates and analyzed by ADAP. An isotype antibody was also tested as a negative control. (b) Antibodies were then spiked into fetal bovine serum and analyzed. (c) Finally, biotin-DNA conjugates bearing alternate sequences were used to show replicability. Error bars represent the standard deviation from triplicate but are too small to be visualized for many data points.

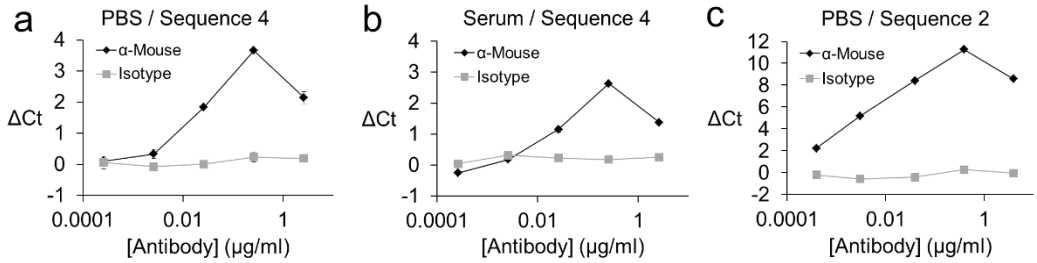

Figure S3. Representative ADAP curves from anti-mouse detection experiment. (a) Anti-mouse antibodies were incubated with mouse IgG-DNA conjugates and analyzed by ADAP. An isotype antibody was also tested as a negative control. (b) Antibodies were then diluted into fetal bovine serum and analyzed. (c) Finally, mouse IgG-DNA conjugates bearing alternate sequences were used to show replicability. Error bars represent the standard deviation from triplicate but are too small to be visualized for many data points.

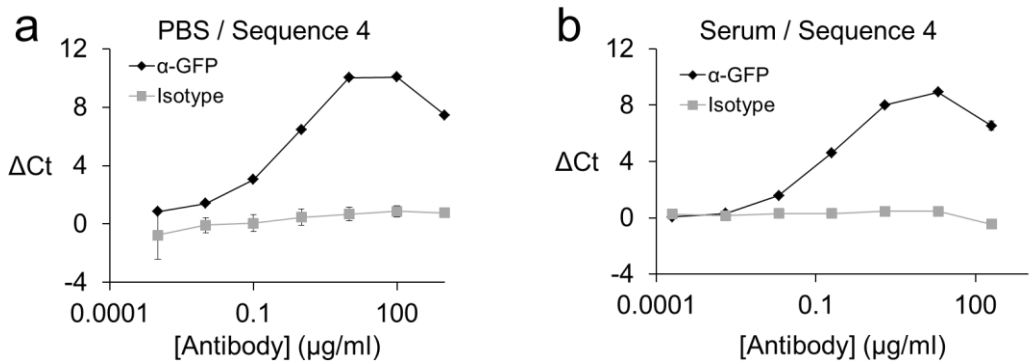

Figure S4. Representative ADAP curves from anti-GFP detection experiment. (a) Anti-GFP antibodies were incubated with GFP-DNA conjugates and analyzed by ADAP. An isotype antibody was also tested as a negative control. (b) Antibodies were then diluted into fetal bovine serum and analyzed. All experiments were performed in triplicate. Error bars represent the standard deviation from triplicate but are too small to be visualized for many data points.

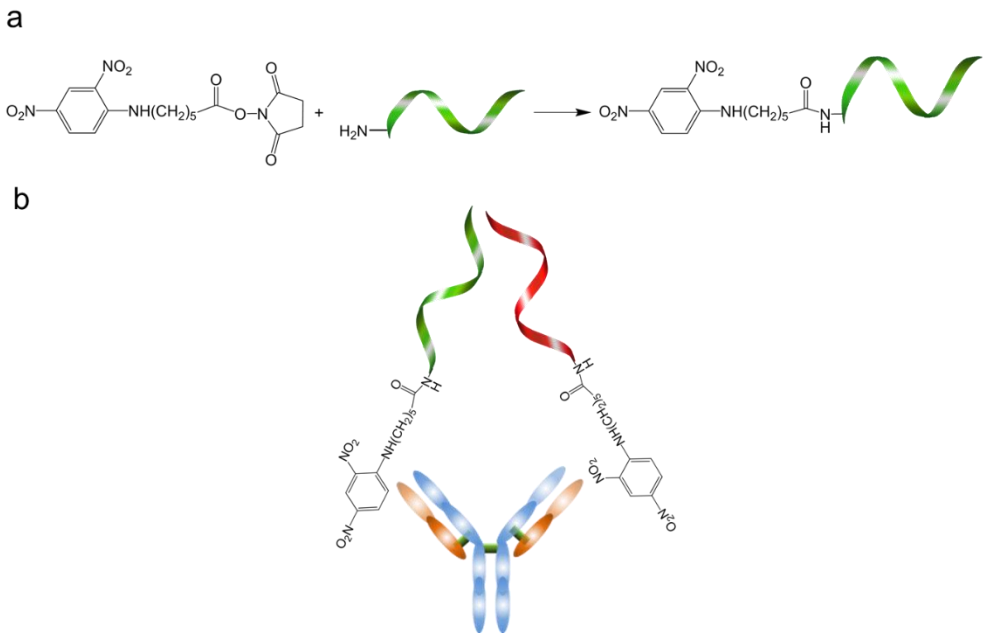

Figure S5. Schematic diagram for small molecule-DNA conjugate ADAP. (a) Reaction scheme for small molecule-DNA conjugate synthesis. DNP-DNA conjugates are synthesized by reacting succinimidyl ester-activated DNP with amine modified DNA in one step. The conjugation product is then characterized by mass spectrometry (b) Small molecule-DNA conjugate pairs are brought in close proximity by binding to the complementary determining region of the

antibodies. A short bridge oligonucleotide hybridizes to the complementary sequences, and a DNA ligase joins the two-halves of DNA into a full length amplicon, which can be further amplified and quantified by qPCR.

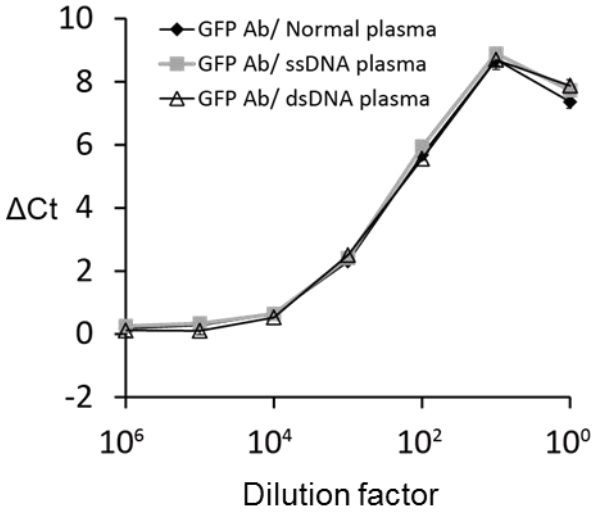

Figure S6. Detection of anti-GFP antibodies in anti-DNA and normal plasma without competition DNA. Anti-GFP antibodies were spiked into both normal plasma and anti-DNA plasma. Serial dilution of the spiked plasma samples were analyzed by ADAP.

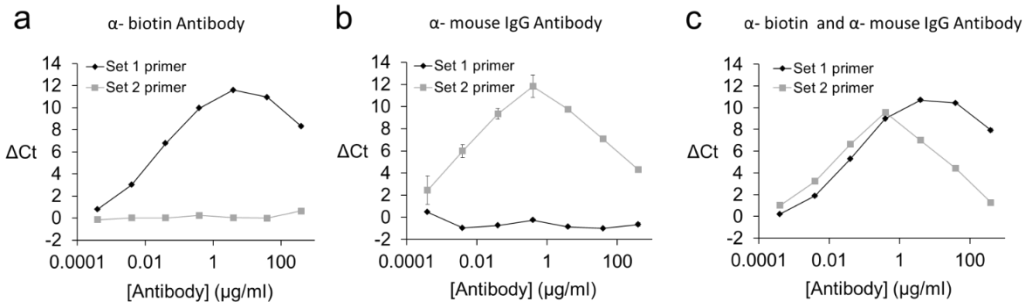

Figure S7. Representative multiplex ADAP curves for multiple antibodies. (a) Both biotin-DNA (Sequence Set 1) conjugates and mouse-IgG-DNA (Sequence Set 2) conjugates are incubated with anti-biotin antibody and analyzed by ADAP using both primer sets. Only sequence 1 shows detectable signals. (b) Both conjugates are incubated with anti-mouse-IgG antibody. Only sequence 2 shows detectable signals. (c) Both biotin-DNA and mouse-IgG-DNA conjugates are incubated with both antibodies. Both sequence set 1 and set 2 show signals. These results demonstrate the orthogonality of multiplexed antibody detection

using ADAP.

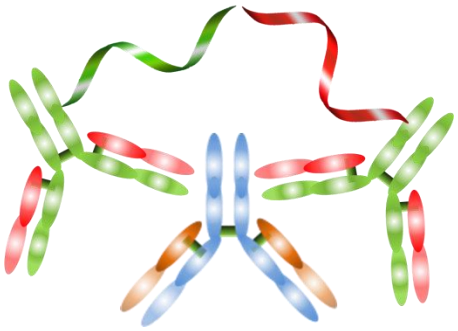

Figure S8. Schematic diagram for proximity ligation assay. In proximity ligation assay, a single batch of polyclonal antibodies can be split into two halves, where each half is conjugated to unique DNA oligonucleotides (green and red). In the presence of the target molecule (in this case an immunoglobulin molecule), the two antibody-DNA conjugates bind to different epitopes on the target molecules and are brought in close proximity. Upon the addition of a bridge oligonucleotide and DNA ligase, the two halves of DNA on the conjugate are linked together and regenerate the full length amplicon, which can be further quantified by qPCR.

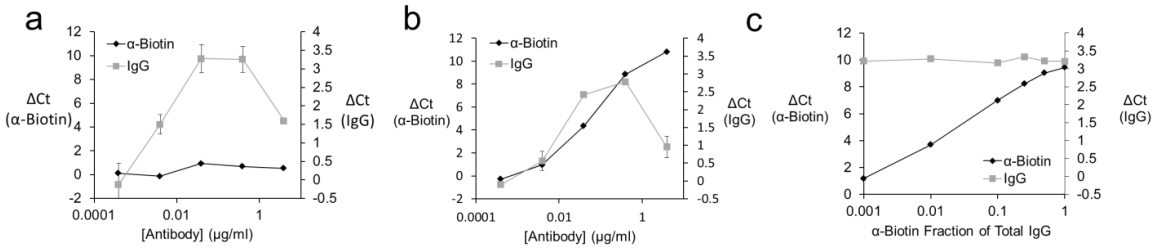

Figure S9. Representative multiplex ADAP and PLA curves for antigen-specific antibodies and total IgG. (a) Both biotin-DNA conjugates (ADAP probes)and anti-goat-IgG-DNA conjugates (PLA probes) are incubated with goat IgG. Only PLA probe shows detectable signals. (b) Both biotin-DNA and anti-goat-IgG-DNA conjugates are incubated with goat anti-biotin antibody. Both ADAP and PLA probes show detectable signals. (c) Both biotin-DNA and anti-goat-IgG-DNA conjugates are incubated with varied fraction of anti-biotin antibodies under fixed total IgG condition. ADAP probes show concentration dependent signals and PLA probes show stable strong signals. These results demonstrate the orthogonality of multiplex antibody and total antibody detection using ADAP

and PLA.

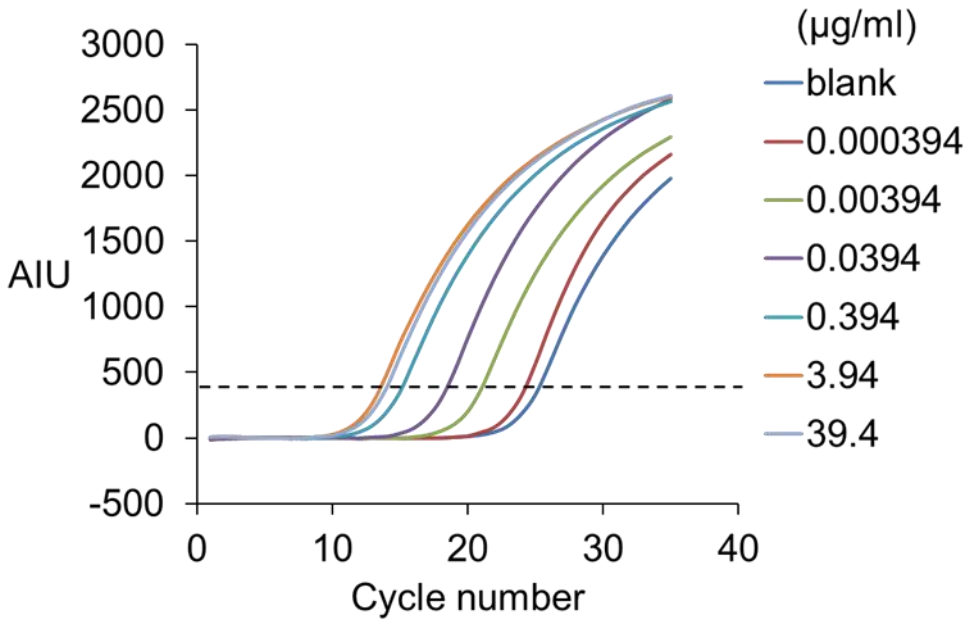

Figure S10. Raw fluorescence data from a representative qPCR ADAP experiment. Serially diluted antibodies are analyzed by ADAP. The threshold fluorescence value is indicated by the dashed line. The Ct value is defined as the cycle number where the fluorescence value corresponds to the threshold value. Amplification curves with higher antibody concentrations reach exponential amplification earlier and thus have smaller Ct values. ΔCt is defined as the Ct value of the blank minus Ct value of the sample. The higher the antibody concentration, the larger the ΔCt value.

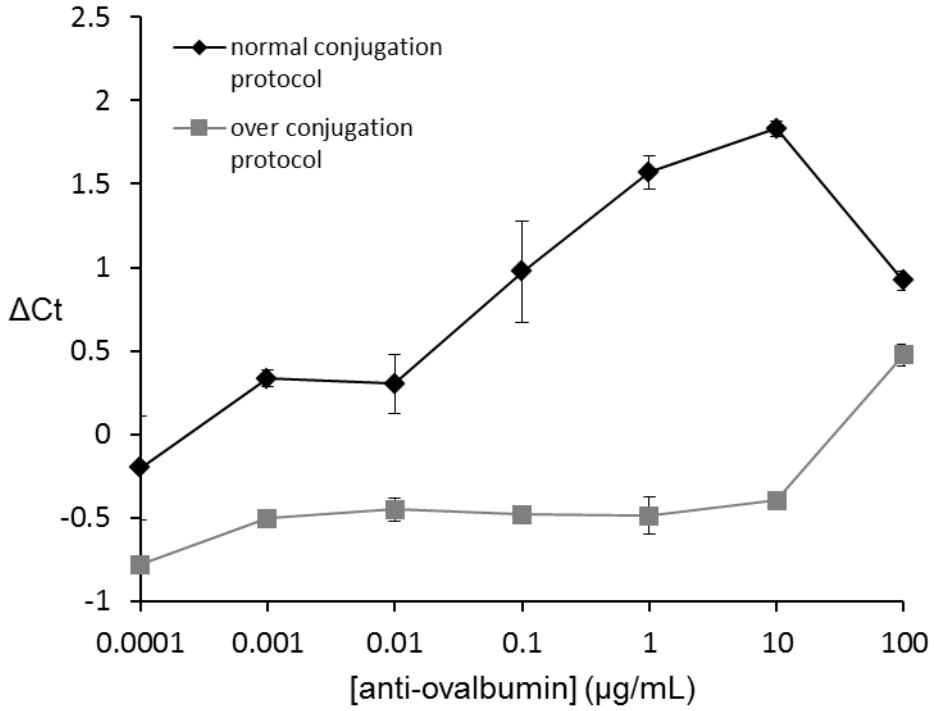

Figure S11. Effect of antigen-DNA conjugation ratio on ADAP performance. Ovalbumin antigens are conjugated to oligonucleotides with either standard or overconjugating protocol, and the DNA-to-antigen ratios are determined to be 1:2 and 1:6 respectively. The ovalbumin conjugates are incubated with dilution series of monoclonal anti-OVA antibodies in buffer and subjected to ADAP analysis. The overconjugated ovalbumin (grey) show significantly reduced assay sensitivity while normal conjugated ovalbumin shows concentration dependent signal as expected. This result can be reasoned by epitope masking when antigens are overconjugated with oligonucleotides.

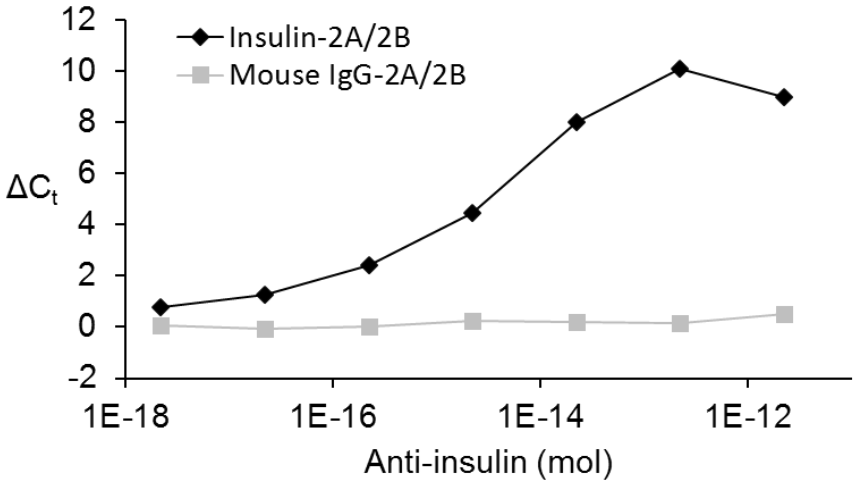

Figure S12. Detection of anti-insulin antibodies in bovine serum by insulin-DNA conjugates and mouse IgG-DNA conjugates. The anti-insulin antibodies do not agglutinate mouse IgG-DNA conjugates and thus no signals are observed. This result demonstrates that ADAP is specific for the cognate antigen-antibody pair.

REFERENCE

1. Bai, T.; Zhou, J.; Shu, Y. Serologic study for influenza A (H7N9) among high-risk groups in China. *N. Engl. J. Med.* **2013**, *368*, 2339-2340.

2. Meroni, P. L.; *et al*. Standardization of autoantibody testing: a paradigm for serology in rheumatic diseases. *Nat. Rev. Rheumatol*. **2014**, *10*, 35–43.

3. Reddy, M. M.; *et al.* Identification of candidate IgG biomarkers for Alzheimer's disease via combinatorial library screening. *Cell* **2011**, *144*, 132-142.

4. Anderson, K. S.; *et al.* Protein microarray signature of autoantibody biomarkers for the early detection of breast cancer. *J. Proteome. Res.* **2011**, *10*, 85-95.

5. Bradford, T.J.; Wang, X.; Chinnaiyan, A.M. Cancer immunomics: using autoantibody signatures in the early detection of prostate cancer. *Urol. Oncol.* **2006***, 24*, 237-242.

6. Kudo-Tanaka, E.; *et al.* Autoantibodies to cyclic citrullinated peptide 2 (CCP2) are superior to other potential diagnostic biomarkers for predicting rheumatoid arthritis in early undifferentiated arthritis. *Clin. Rheumatol.* **2007**, *26*, 1627-1633.

7. Liu, E.; Eisenbarth, G.S. Accepting clocks that tell time poorly: fluid-phase versus standard ELISA autoantibody assays. *Clin. Immunol*. **2007**, *125*, 120–126.

8. Butler, J.E.; *et al*. The immunochemistry of sandwich ELISAs—VI. Greater than 90% of monoclonal and 75% of polyclonal anti-fluorescyl capture antibodies (CAbs) are denatured by passive adsorption. *Mol. Immunol.* **1993**, *30*, 1165-1175.
9. Z hang, B.; Kumar, R. B.; Dai, H.; Feldman, B. J. A plasmonic chip for biomarker discovery and diagnosis of type 1 diabetes. *Nat. Med.* **2014**, *20*, 948-953.
10. Greenbaum, C. J.; Palmer, J. P.; Kuglin, B.; Kolb, H. Insulin autoantibodies measured by radioimmunoassay methodology are more related to insulin-dependent diabetes mellitus than those measured by enzyme-linked immunosorbent assay: results of the fourth international workshop on the standardization of insulin autoantibody measurement. *Clin. Endocrinol. Metab.* **1992***, 74*, 1040-1044.
11. Gentile, F.; Conte, M.; Formisano, S. Thyroglobulin as an autoantigen: what can we learn about immunopathogenicity from the correlation of antigenic properties with protein structure. *Immunology* **2004**, *112*, 13-25.
12. Spencer, C. A. Clinical utility of thyroglobulin antibody (TgAb) measurements for patients with differentiated thyroid cancers (DTC). *J. Clin. Endocrinol. Metab.* **2011***, 96*, 3615-3627.
13.Mahler, M.; Fritzler, M. J. Epitope specificity and significance in systemic autoimmune diseases. *Ann. N.Y. Acad. Sci.* **2010**, *1183*, 267-287.
14. Robinson, W. H.; *et al*. Autoantigen microarrays for multiplex characterization of autoantibody responses. *Nat. Med.* **2002***, 8*, 295-301.
15. Simon-Vecsei, Z.; *et al.* A single conformational transglutaminase 2 epitope contributed by three domains is critical for celiac antibody binding and effects*. Proc. Natl. Acad. Sci. U.S.A.* **2011**, *109*, 431-436.
16. Richter, W.; Shi, Y.; Baekkeskov, S. Autoreactive epitopes defined by diabetes- associated human monoclonal antibodies are localized in the middle and C-terminal domains of the smaller form of glutamate decarboxylase. *Proc. Natl. Acad. Sci. U.S.A.* **1993***, 90*, 2832-2836.
17. Iverson, G. M.; Matsuura, E.; Victoria, E. J.; Cockerill, K. A.; Linnik, M. D. The orientation of beta2GPI on the plate is important for the binding of anti-beta2GPI autoantibodies by ELISA. *J. Autoimmun.* **2002**, *18*, 289-297.
18.Silva, F.; Hummel, A. M.; Jenne, D. E.; Specks, U. Discrimination and variable impact of ANCA binding to different surface epitopes on proteinase 3, the Wegener's autoantigen. *J. Autoimmun.* **2010**, *35*, 299-308.
19. Adler, S. P.; *et al*. Detection of cytomegalovirus antibody with latex agglutination. *J. Clin. Microbiol*. **1988**, *26*, 2116-2119.

20. Fredriksson, S.; *et al.* Protein detection using proximity-dependent DNA ligation assays*. Nat. Biotechnol.* **2002**, *20*, 473-477.
21. Söderberg, O.; *et al*. Direct observation of individual endogenous protein complexes *in situ* by proximity ligation. *Nat. Methods*. **2006**, *3*, 995-1000.
22. Yu, L.; *et al.* Distinguishing persistent insulin autoantibodies with differential risk*. Diabetes* **2012**, *61*, 179-186.
23. Romano, A.; *et al.* IgE-mediated hypersensitivity to cephalosporins: cross-reactivity and tolerability of penicillins, monobactams, and carbapenems. *J. Allerg. Clin. Immunol.* **2010**, *126*, 994-999.
24. Kaur, J.; Boro, R. C.; Wangoo, N.; Singh, K. R.; Suri, C. R. Direct hapten coated immunoassay format for the detection of atrazine and 2, 4-dichlorophenoxyacetic acid herbicides. *Anal. Chim. Acta.* **2008***, 607*, 92–99.
25. Stassi, G.; De Maria, R. Autoimmune thyroid disease: new models of cell death in autoimmunity. *Nat. Rev. Immunol*. **2002**, *2*, 195-204.
26. Riboldi, P.; *et al.* Anti-DNA antibodies: a diagnostic and prognostic tool for systemic lupus erythematosus? *Autoimmunity* **2005**, *38(1)*, 39-45.
27. Ruffatti, A.; *et al.* Anti-double-stranded DNA antibodies in the healthy elderly: prevalence and characteristics. J Clin Immunol. **1990**, *10*, 300-303.
28. Kumar, V.; *et al.* Celiac disease and immunoglobulin A deficiency: how effective are the serological methods of diagnosis? *Clin. Diag. Lab Immunol.* **2002**, *9*, 1295-1300.
29. Roche, A. M.; Richard, A. L.; Rahkola, J. T.; Janoff, E. N.; Weiser, J. N. Antibody blocks acquisition of bacterial colonization through agglutination. *Mucosal Immunology* **2015**, *8*, 176-185.
30. Fernando, S. A.; Wilson, G. S. Studies of the 'hook' effect in the one-step sandwich immunoassay. *J. Immunol. Methods* **1992**, *151*, 47-66.
31. Kricka, L. Human anti-animal antibody interferences in immunological assays. *J. Clin. Chem.* **1999**, *45*, 942-956.
32. Faraoni, S.; *et al*. Evaluation of a rapid antigen and antibody combination test in acute HIV infection. *J. Clin. Virol.* **2013**, *57*, 84-87.
33. Yang, T.; Zhong P.; Qu, L.; Wang, C.; Yuan, Y. Preparation and identification of anti-2, 4-dinitrophenyl monoclonal antibodies. *J Immunol Methods*. **2006**, *313(1-2)*, 20-28.
34. Chipinda, I.; Hettick, J. M.; Siegel, P. D. Haptenation: chemical reactivity and protein binding. *J Allergy*. **2011**, *2011*, 839682.
35. Ling D.; Salvaterra P. M.; Robust RT-qPCR data normalization: validation and selection of internal reference genes during post-experimental data analysis. *PLoS One* **2011**, *6(3)*, e17762.

36. Ochert A.S., Boulter A.W., Birnbaum W., Johnson N.W., Teo C.G. Inhibitory effect of salivary fluids on PCR: potency and removal. *PCR Methods Appl*. **3(6)**. 365-368 (1994).
37. Ji, Y. T.; Qu, C. Q.; Cao, B. Y. An optimal method of DNA silver staining in polyacrylamide gels. *Electrophoresis* **2007**, *28*, 1173-1175.
38. Netzel, B. C.; *et al.* Thyroglobulin (Tg) testing revisited: Tg Assays, TgAb assays, and correlation of results with clinical outcomes. *J Clin Endocrinol Metab.* **2015***, 100*, 1074-1083.
39. Niemeyer, C.; Adler, M.; Wacker, R. Detecting antigens by quantitative immuno-PCR*. Nat. Protoc*. **2007**, *2*, 1918-1930.
40. Findlay, J. W. A.; Dillard, R. F. Appropriate calibration curve fitting in ligand binding assays. *AAPS J.* **2007**, *9*, 260-267.
41. Armbruster, D. A.; Pry, T. Limit of blank, limit of detection and limit of quantitation. *Clin. Biochem. Rev.* **2008**, *29*, S49-S52.
42. Bastarache, J. A.; *et al*. Accuracy and reproducibility of a multiplex immunoassay platform: a validation study. *J. Immunol. Methods* **2011**, *367*, 33–39.

Chapter 3
Application of antibody detection by agglutination-PCR (ADAP) for early detection of HIV infection using oral fluids

Chapter 3. Application of antibody detection by agglutination-PCR (ADAP) for early detection of HIV infection using oral fluids*

In this chapter, I will describe a selective application of ADAP, wherein ADAP has proven to be more effective than current options in clinical settings. The principal and concept established in this chapter should render ADAP widely applicable to many other diseases.

*Peter Robinson, PhD contributes significantly to results presented in this chapter. The content in this chapter has been published at PNAS, 2018.

Antibody detection by agglutination–PCR (ADAP) enables early diagnosis of HIV infection by oral fluid analysis, Proceedings of the National Academy of Sciences, 2018

INTRODUCTION

Eliminating human immunodeficiency virus (HIV) from the human population will require innovative diagnostic and therapeutic strategies (1). To this day, large-scale screening efforts remain the most effective public health mechanism to identify and treat HIV-infected people (1). Early identification of newly-infected individuals permits the timely initiation of anti-retroviral therapy (ART) to reduce transmission rates and improve health outcomes (1). During this “acute” period immediately following infection, patients are up to 26-times more infectious and over 50% of new transmissions are thought to occur in this window (2, 3).

While blood-based assays efficiently diagnose HIV infection during the acute phase, these tests suffer from poor compliance rates due to their invasive nature (4, 5). In contrast, non-invasive assays such as oral fluid (OF) antibody tests enjoy high levels of compliance, but lack the analytical sensitivity to detect very low levels of antibodies in the OF of acutely infected individuals (6-10). Currently, no existing test meets the pressing medical need to non-invasively detect HIV during acute infection, which is essential to maximize the number of people screened and to intervene at the earliest time.

HIV tests that analyze easily-collected OF increase the numbers of individuals tested in situations where needle-mediated blood drawing is inefficient or unsafe (4, 5). The use of oral specimens has facilitated the testing of many populations including: (a) populations for whom it is inconvenient or unsafe to test using needles (e.g. prisons); (b) patients whose veins are difficult

to draw from (e.g. drug users, infants); and (c) people who do not wish to have their blood drawn using needles (e.g., children, adolescents) (10-12). Furthermore, antibodies in OF are stable for several weeks at ambient temperature, thus decreasing the likelihood of false results when cold chain shipping is not available (13, 14). Finally, OF is much safer to handle on a large scale, as HIV cannot be transmitted by OF thanks to significantly lower viral loads and the presence of naturally-occurring enzymes and other inhibitors that deactivate the virus (15). OF therefore represents an ideal sample type for large-scale screening of HIV incidence in many groups.

Antibodies are the most reliable markers of HIV infection in OF (16). While HIV-derived RNA and proteins (i.e., p24) are considered powerful blood-borne markers for detecting early infections, these HIV components do not consistently appear in OF (16). Thus, assays that measure HIV RNA by quantitative PCR (qPCR) or HIV protein (p24) by enzyme-linked immunoassays (EIA) are unsuitable for OF screening. By contrast, HIV-associated immunoglobulins are reliable markers of infection in OF (17, 18). Indeed, detection of OF IgG in EIA-type formats forms the basis of the FDA-approved OraQuick test. Unfortunately, however, this test cannot detect disease until at least 40 days after infection (18). This unacceptably long window period is attributed in part to the 1,000-fold lower antibody concentration in OF relative to serum/plasma (20). As a point of comparison, blood-based tests can detect infection as soon as 14-25 days after exposure (19). The diminished antibody titers along with much lower antibody production in the early phase of the disease pose significant analytical challenges for current HIV OF antibody tests (20).

Here we report an ultrasensitive OF HIV antibody detection method based on Antibody Detection by Agglutination-PCR (ADAP) technology (**Fig. 1**) (21). The ADAP platform, similar in nature to proximity ligation assay (PLA) (23), leverages multivalent binding of antibodies to drive the agglutination of antigen-DNA conjugates. The induced proximity enables ligation of DNA fragments to form a full-length DNA amplicon, which can then be quantified by qPCR. As reported previously, this amplification permits detection of antigen-specific antibodies at high zeptomole levels in 1 μL samples (21). Since ligation is only triggered following a productive antibody-antigen interaction, ADAP does not require washing steps to remove unbound antigen-DNA conjugates and is thus well-equipped to detect low-affinity antibodies. Furthermore, ADAP can detect antibodies of any isotype, including IgM, the earliest antibody marker of acute infection (19). Importantly, DNA barcoding allows multiplexing by linking the

identity of each antibody to a unique DNA sequence. Thus, antibodies specific for multiple antigens can be detected in a single sample.

Accordingly, we developed an HIV OF test based on ADAP using DNA conjugates of the HIV proteins p24, gp41 and gp120 (**Fig. 1A**), the standard antigens for clinical HIV antibody testing (22). The ADAP test was found to be 1,000-10,000-fold more sensitive than the EIA used in clinical settings. We analyzed OF samples from the Alameda County (California) Public Health Laboratory's HIV screening program. We confirmed previously assigned HIV diagnoses with 100% accuracy. To further evaluate the assay, we tested a panel of 8 OF samples that were classified as "indeterminate" by current assays. ADAP analysis re-classified 6 of these samples as HIV positive due to the presence of two or more anti-HIV antibodies. Critically, one such patient was confirmed to be HIV-infected by a follow-up blood test. Thus, ADAP-based HIV testing may enable population-based screening for early HIV infection using OF.

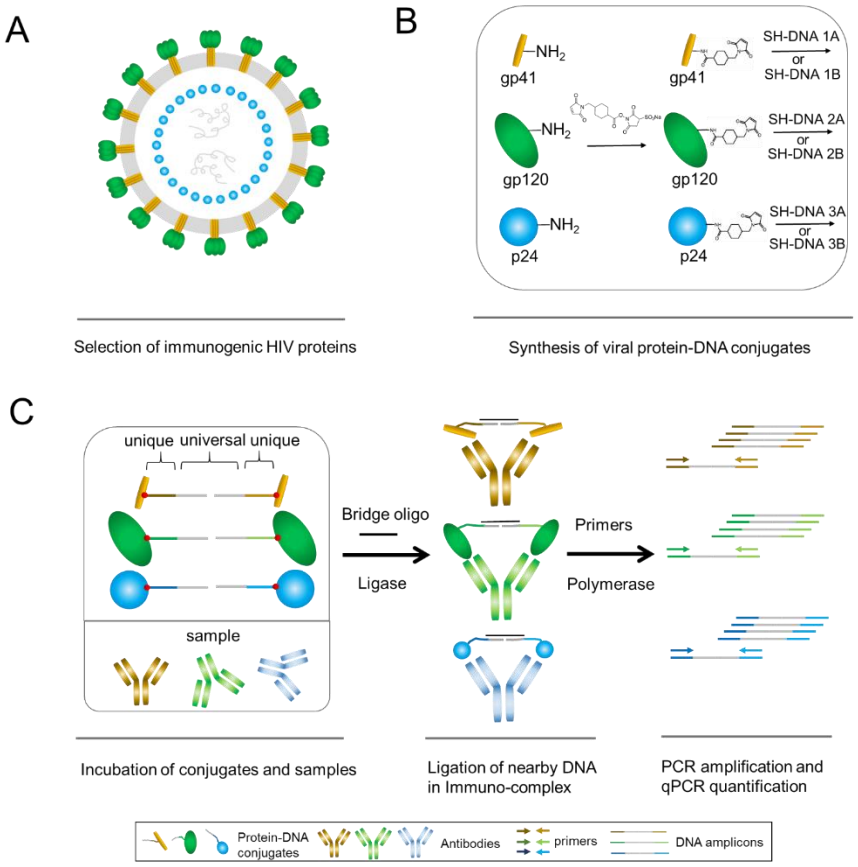

Figure 1. Principle scheme of antibody-detection by agglutination-PCR (ADAP) for HIV diagnosis. A, HIV virus contains many immunogenic proteins including envelope glycoprotein gp160, which can be cleaved into gp41 (brown) and gp120 (green), and viral capsid protein p24 (blue). B, Recombinant proteins of

these selective viral components are activated by installation of small molecule cross-linker sulfo-SMCC onto lysine residues, and react with thiol-functionalized DNA by Michael addition reaction to form protein-DNA conjugates. C, Upon incubation with samples, antibodies and conjugates form immuno-complexes, wherein nearby DNA can be ligated into a full length amplicon by a universal bridge oligonucleotides and DNA ligase. Finally, each amplicon bears unique primer binding site for independent amplification and quantification by real-time quantitative PCR (qPCR). Critically, DNA conjugate alone without ligation is PCR-incompetent since it only bears one primer binding site. Only after successful reconstitution into a full length amplicon would it be exponentially amplifiable by PCR. This “turn-on” mechanism allows ADAP to leverage PCR’s analytical sensitivity while reserve assay’s specificity.

RESULTS

Synthesis of viral antigen-DNA conjugates.

We used commercially-available full-length recombinant p24, gp120 and gp160 (precursor of gp41 and gp120), all from HIV-1 clade C as substrates for DNA conjugation (**Fig. 1A**). For gp41, we instead used a recombinant gp41-derived peptide fragment. We then synthesized the antigen-DNA conjugates by lysine modification with sulfosuccinimidyl 4-(N-maleimidomethyl)-cyclohexane-1-carboxylate (sulfo-SMCC), followed by reacting the newly installed maleimide groups with thiolated oligonucleotides that had been pre-reduced by treatment with dithiothreitol (DTT) (**Fig. 1B**). Unreacted reagents were removed by extensive purification with size-exclusion filter columns. Viral antigen-DNA conjugation ratios were determined by UV-Vis spectroscopy and gel analysis (**Fig. S1**). The conjugates were then diluted in buffer and stored at 4 °C until use. Importantly, in a singleplex experiment, all viral antigen-DNA conjugates contained the same DNA sequence (**Table S1**), whereas in the multiplex experiment, each viral antigen-DNA conjugate had a unique DNA sequence (**Table S1**).

ADAP workflow for HIV antibody detection.

In an ADAP experiment, pairs of viral antigen-DNA conjugates were first diluted in buffer. One antigen-DNA conjugate bore the 5’ half of a PCR amplicon while the other conjugate bore the 3’ half that was 5’ phosphorylated to enable ligation. The pooled conjugates were added to 1 µL of OF sample and incubated for 30 min to allow antibody binding. Next, DNA ligase and a bridging oligonucleotide were added and incubated for 15 min. The ligation mixture was

then pre-amplified by PCR and the resulting products were quantified by qPCR (**Fig. 1C**). As high Ct values of qPCR were associated with low assay reproducibility, we included a pre-amplification step in the ADAP protocol to ensure high assay reproducibility as reported previously (21, 23).

ADAP showed enhanced analytical sensitivity compared to a standard OF EIA used in public health labs.

To demonstrate that viral antigen-DNA conjugates were capable of detecting their cognate antibodies, we obtained a panel of highly-purified human antibodies against p24, gp41 and gp160 derived from HIV patients (Immunodx). We then serially diluted each HIV antibody into buffer and quantitated them using ADAP or a clinical EIA (Avioq microelisa, FDA approved). We observed a concentration-dependent signal for all three antibodies using ADAP with dynamic range up to 105 (**Fig. 2**). The detection limits were 110, 880 and 550 zeptomoles (10-21 moles) of anti-p24, anti-gp41 and anti–gp160, respectively. In contrast, with the EIA assay, the detection limits were 8.5, 9.2 and 11 femtomoles for anti-p24, anti-gp41 and anti-gp160, respectively. Collectively, ADAP shows 1,000-10,000-fold enhanced analytical sensitivity compared to a clinical EIA assay.

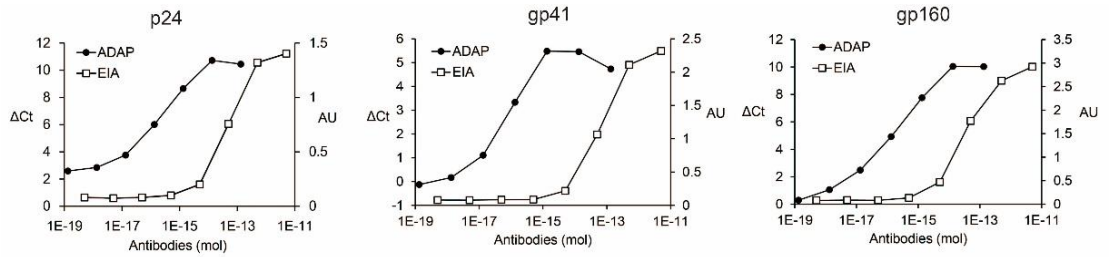

Figure 2. ADAP's analytical sensitivity outperformed commercial EIA by several orders of magnitude. Purified human anti-HIV antibodies were serially diluted in buffer. The dilution series were assayed by ADAP and EIA (Avioq microelisa). The x-axis was the amount of antibody, while the left y-axis was the signal from an ADAP qPCR experiment and right y-axis was signal from commercial EIA. For most data point, the error bar were too small to be visualized.

Singleplex clinical sensitivity and specificity using archived OF samples from a public health screening program.

Next, we evaluated the clinical sensitivity and specificity of the ADAP method using OF samples obtained as part of an HIV screening effort by the Alameda County (California) Public Health Laboratory. We selected 22 EIA-

reactive (“positive”) OF samples from HIV-infected patients and 22 EIA-non-reactive (“negative”) OF samples from non-HIV donors. The positive OF samples were selected to represent a range of EIA assay signal intensities, with signal-to-cutoff ratios from 1.7-6.7 measured by EIA (Avioq microelisa). A confirmatory Western blot assay (Orasure) was also performed on the OF samples to ensure the presence of two or more reactive antibodies, as recommended by Centers for Disease Control and Prevention (CDC) guidelines (24).

We incubated the OF samples with each viral antigen-DNA conjugate (p24, gp41, gp120 and gp160) and followed the ADAP protocol as outlined above. For all four viral antigens, a clear difference ($P < 0.05$) between positive and negative OF was observed (**Fig. 3A**). We then used two standard deviations of negative OF to establish a positivity threshold for each antibody marker. We defined HIV positivity as two or more antibodies with signal intensities above threshold values. Under these stringent criteria, all 22 “negative” OF samples were correctly classified as HIV-negative and all 22 “positive” OF samples were classified as HIV-positive, achieving 100% sensitivity and specificity (**Fig. 3A**). Additionally, we sought to compare the signal intensities measured using the ADAP and clinical EIA assays (Avioq microelisa). The EIA assay measured total antibody-derived signal. To approximate this composite measurement, we summed the ADAP signal intensities derived from three viral antigens (p24, gp41, gp120, **Fig. 3B**). As shown in Fig. 3C, the correlation between the two assays was high ($R=0.80$, $P < 0.05$). Signal correlations of individual HIV components to EIA were shown in **Fig. S4**. These results further validated ADAP as a means to detect anti-HIV antibodies.

A final concern we sought to address was whether the difference in signal between HIV-positive and HIV-negative individuals was simply the result of intrinsic differences in their OF compositions. For example, OF from immunosuppressed HIV-positive patients might contain unknown factors that elevated ADAP signal intensity in an antibody-independent manner. To preclude this possibility, we synthesized a negative-control GFP (green-fluorescent protein)-DNA conjugates. As there were no naturally-occurring anti-GFP antibodies within human OF, we expected that no signal should be observed from ADAP analysis using GFP-DNA conjugates. Indeed, HIV-positive and HIV-negative OF were indistinguishable following ADAP analysis with GFP-DNA conjugates ($P=0.5$) (**Fig. S2**). This experiment supports the assignment of signals such as those shown in Figs. 3A and 3B to the presence of anti-HIV antibodies in OF.

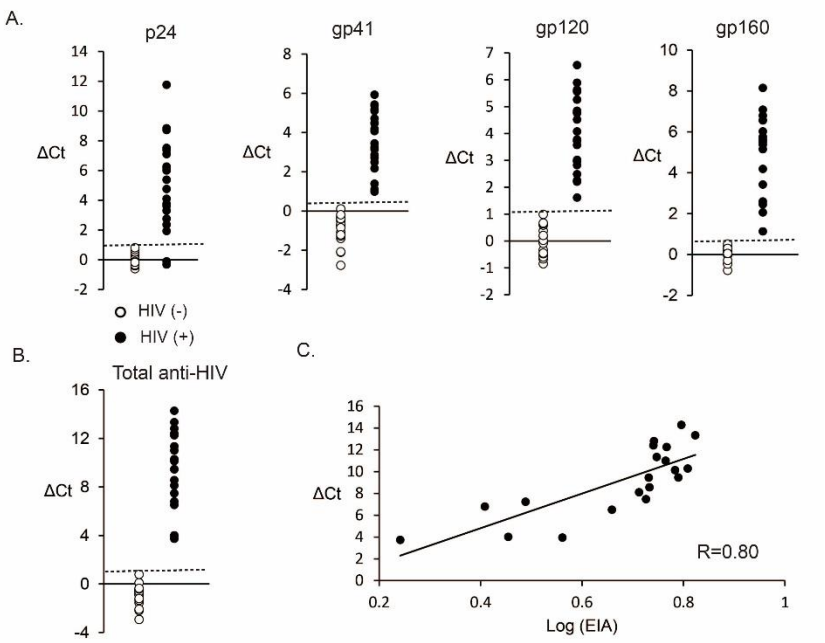

Figure 3. Singleplex ADAP analysis of oral fluid samples. A, Oral fluid samples from HIV-negative (n=22) and HIV-positive (n=22) patients were analyzed by ADAP. Using cutoff values established from HIV-negative samples, HIV-positive samples showed 91% positivity for p24 and 100% for gp41, gp120 and gp160. B, Cumulative signal from all anti-HIV antibodies. All 22 HIV-positive samples showed higher signal than 22 HIV-negative samples. By defining positivity as the presence of two or more HIV antibodies, singleplex ADAP analysis yields 100% clinical sensitivity and specificity in comparison to the clinical gold-standard EIA. C, The cumulative signal intensities of ADAP correlated well to the signal intensities of EIA (R = 0.80, P<0.05).

Multiplex clinical sensitivity and specificity using archived OF samples from a public health screening program.

Our previous experiments showed that ADAP faithfully detected individual HIV-specific antibodies from OF. Next we sought to create a multiplexed ADAP assay to simultaneously analyze three of these antibodies in a single test. We synthesized each viral antigen-DNA conjugate with unique DNA barcodes (**Fig. 1B and Table S1**). Only the correct antibody markers would agglutinate the related antigen-DNA conjugates, leading to amplification of the associated barcodes. Unique primer pairs within different wells of a qPCR plate could then be used to quantify the amount of each DNA barcode (**Fig. 1C**).

We re-analyzed the 22 “positive” OF and 22 “negative” OF samples using

this multiplexed ADAP strategy for antibodies against p24, gp41 and gp120 in a single assay. Gp160 was not included due to the fact that gp41 and gp120 are the cleavage products of gp160. These two antigens together cover the entire amino acid sequence of gp160. Thus, the use of p24, gp41 and gp120 should yield a near-complete landscape of the antibody response to HIV infection. As before, we defined HIV-positivity by detection of two or more antibodies above a cutoff threshold. By this metric, a clinical profile identical to our previous singleplex analysis was obtained, with clinical sensitivity and specificity of 100% (**Fig. 4**). We observed the same patterns for individual antigens, with 91% positivity for anti-p24, and 100% for anti-gp41 and anti-gp120 (**Fig. 4**). Correlations of signals between singleplex and multiplexed experiments were also very high (R = 0.99 for p24, 0.97 for gp41 and 0.95 for gp120) (**Fig. 5**).

These data demonstrated that ADAP detection of HIV antibodies in OF was at least as sensitive and specific as a current clinical standard assay employed in public health labs. Importantly, the ADAP OF assay allowed multiplexed profiling of the HIV immune response in a single assay.

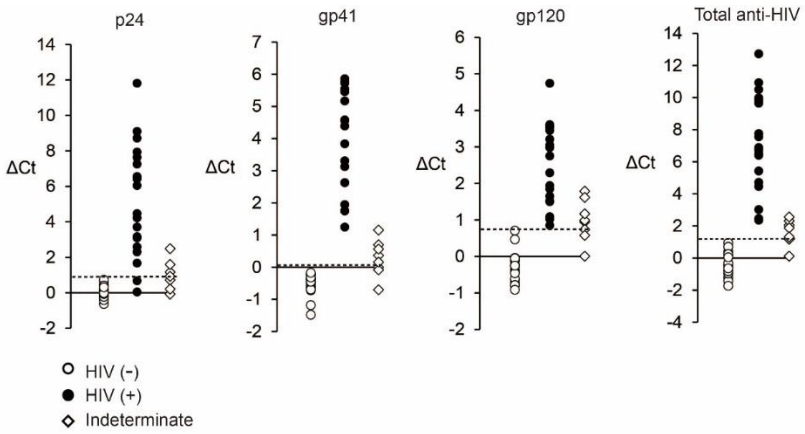

Figure 4. Multiplex ADAP analysis of clinical oral fluid samples. A multiplex version of ADAP simultaneously detected antibodies against p24, gp41 and gp120. We re-analyzed the oral fluid samples from before, and observed identical performance to the singleplex analysis. HIV-positive samples again showed 91% positivity in p24, 100% for gp41 and gp120. Applying the same criteria for positivity (2 or more antibodies), multiplex ADAP analysis demonstrated 100% clinical sensitivity and specificity as seen with singleplex. In addition, we analyzed several “indeterminate” oral fluid samples (n=8) with multiplex ADAP. Detailed ADAP analysis results for 8 indeterminate samples were summarized in Table I.

ADAP may detect HIV earlier than current OF assays

Finally, we performed a pilot study to determine whether ADAP analysis of OF could detect HIV infection earlier than the clinical OF assay (Avioq Microelisa). We obtained a panel of 8 OF samples that showed indeterminate results using the current OF test. The indeterminate status was defined by signal-to-cutoff values measured by EIA (Avioq microelisa) between 0.6-0.9 and showed single weak band in western blot (Orasure). OF samples that met these criteria display “HIV-positive-like” qualities, but did not meet the full criteria for HIV positivity. These samples might be derived from patients in the early seroconversion phase of HIV infection, and thus might harbor very low levels of antibodies that traditional assays could not detect.

ADAP analysis revealed that 6 of 8 indeterminate samples were positive for two or more HIV-associated antibodies, and thus re-classified these patients as HIV-positive (**Fig. 4 and Table I**). Critically, we obtained a blood sample from one ADAP-positive/EIA-indeterminate individual (follow-up blood samples were not available for other indeterminate individuals). As blood contains 1,000-fold higher levels of antibodies compared to OF, current tests can analyze such samples with improved confidence. Analysis of this blood sample revealed the patient to be HIV-positive, in agreement with ADAP’s classification. These results suggested that ADAP’s enhanced analytical sensitivity might enable early detection of HIV infection from OF.

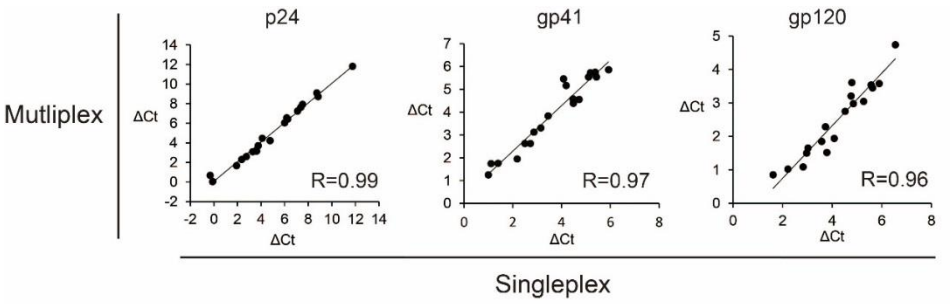

Figure 5. **Singleplex and multiplex ADAP signal intensities showed strong correlation**. The signal intensities from singleplex and multiplex ADAP analysis of the same samples were plotted and analyzed for correlation. Correlation coefficients of 0.99, 0.97 and 0.96 were observed for p24, gp41 and gp120 respectively.

DISCUSSION

Since the first FDA–approved tests for detection of HIV antibodies became

available in 1985 (26), assays for blood-based HIV diagnostics have evolved enormously. The first-generation HIV serum assays used whole HIV lysates as antigens, with anti-human-IgG secondary antibodies as reporters. This assay design suffered from low specificity due to contaminants present in the lysates (24). To address this problem, a second-generation assay instead employed recombinant peptides and proteins to improve the purity of antigen probes. However, second-generation assays still required a long period of up to 40 d after exposure before antibody detection was possible (24). A third-generation assay sought to improve the window period by detecting both IgM and IgG anti-HIV antibodies in a sandwich EIA format (24). Since IgM antibodies appear much earlier than IgG in the seroconversion process, this technology shortened the window period to approximately 20-25 d. Finally, fourth-generation assays not only detected IgM and IgG anti-HIV antibodies, but also detected viral protein p24, which allowed HIV diagnosis approximately 14-16 d after infection (24). In addition to these protein detection assays, HIV RNA assays have been developed to accurately quantify viral loads at the earliest stage of infection (24). Moreover, highly sensitive immunoassays including digital ELISA has also been reported to enable early diagnosis of HIV (25). These innovations together have greatly improved the sensitivity and specificity of HIV diagnosis by blood samples.

IND ID	p24	gp41	gp120	Status
13AC6953	**0.9254**	**0.3633**	**1.785**	Pos
13AC9465	**1.1654**	**1.1533**	**1.615**	Pos
14AC10527	-0.0746	**0.6933**	**0.945**	Pos
14AC7304	0.7154	-0.7067	0.005	Neg
15AC4639	**1.5954**	-0.0067	**0.985**	Pos
15AC8637	0.2054	-0.0867	**1.165**	Neg
16AC1148	**0.9254**	**0.5633**	**0.735**	Pos
16AC6294	**2.4854**	**0.1533**	0.575	Pos
Cutoff	0.75622	0.12831	0.70333	

Table I. Multiplex ADAP assay identified HIV infection missed by commercial EIA. Six out of eight “indeterminate” oral fluid samples were re-classified as HIV positive by multiplex ADAP analysis. Strikingly, a follow-up blood draw confirmed one such sample (16AC6294) to be HIV infected, which was otherwise missed by commercial EIA (Bold font for positive signals).

In contrast, OF-based HIV assays have remained relatively stagnant, with window periods persisting at 40-50 d post-infection. Counterintuitively, the

diagnostic technology used in first- and second-generation blood-based assays outperforms more recent-generation assays when analyzing OF (20). The much lower antibody concentration and inconsistent presence of viral proteins or RNA in OF samples surely contribute to this problem (20). As OF-based assays could greatly improve HIV screening rates and compliance, there remains an unmet need for new and improved OF assays to advance HIV management.

Our ADAP OF assay leveraged the analytical sensitivity of PCR to achieve highly sensitive, specific and multiplex detection of antibodies against several HIV antigens with low sample consumption. Notably, the ADAP test reported on the presence of both IgGs and IgMs, the earliest antibody infection marker, as both species would agglutinate DNA-conjugated antigens (**Table S2**). We demonstrated that our ADAP assay was 1,000-10,000x more sensitive than a standard clinical OF EIA test. The potential clinical utility of this sensitivity was demonstrated by identifying an HIV infection that was otherwise missed by current OF tests.

These results established the basis for further development and validation of ADAP HIV OF assays. First, most viral antigens employed in this report were derived from HIV-1 clade C. These antigens were well-suited to develop assays for centers at the front lines of the HIV pandemic, including South Africa (27). We envisioned our ADAP HIV OF assays best applied as an incidence screening test for public health applications. As such, future experiments should focus on whether ADAP HIV OF assays retain clinical sensitivity and specificity for HIV-1 of other clades. Second, specific antigens for HIV-1 group N, O, P and HIV-2 (e.g. gp36) were not incorporated into current multiplexed panels (28). Including these antigens would strengthen an ADAP assay for HIV diagnosis. Third, we demonstrated a promising but preliminary example of ADAP's ability to detect HIV during the acute infection phase, where other tests might fail. Analysis of paired OF and blood samples throughout the seroconversion processes would be required to show that ADAP assays have a shorter window period in comparison to other assays. Still, ADAP's potential to detect HIV infection using readily-acquired OF samples and a simple qPCR machine should spur the adoption of this test for applications in public health.

METHODS

Materials.

Chemicals were purchased from Sigma Aldrich unless otherwise specified. Dithiothreitol (DTT) and sulfo-SMCC were purchased from Life technologies.

DNA ligase was purchased from EpiCentre (#A8101). Platinum Taq polymerase (#10966026) and SYBR qPCR 2X master mix (#4385610) was purchased from Thermo Fischer. Other reagents were detailed in the method sections as appropriate.

Synthesis of protein-DNA conjugates.

The p24 (Immunodx), gp120 (Immunodx) and gp160 (Avioq) antigens in this study were full length recombinant proteins. The gp41 antigen was a recombinant peptide fragment (Fitzgerald Industry International). The above proteins were suspended in reaction buffer (55 mM sodium phosphate, 150 mM sodium chloride, 20 mM EDTA, pH 7.2) to make 1 mg/mL solutions. Sulfo-SMCC (Thermo Scientific) (1 µL of 8 mM solution in anhydrous DMSO) was added to 10 µL of the protein solution. The reaction mixture was incubated at room temperature (RT) for 2 h. Thiolated-DNA (IDT) was suspended in reaction buffer to 100 µM. A 3 µL of thiolated-DNA solution and 4 µL of 100 mM solution of DTT were mixed to reduce potentially dimerized thiolated-DNA to monomer form. The solution was then incubated at 37 °C for 1 h. The excess sulfo-SMCC in protein mixtures and DTT in thiolated-DNA were removed by 7K MWCO zeba spin column (Thermo Fischer). The thiolated-DNA and viral protein solutions were then pooled and incubated overnight at 4 °C. The DNA-to-protein incubation ratio was 3-to-1 for all proteins and peptides used in this study. Finally, protein-DNA conjugates were purified by 30K MWCO filter (Millipore). Conjugate concentrations were determined by BCA assay (Life Technologies). Conjugation efficiencies were analyzed by SDS-PAGE and silver staining as described previously (21). A representative silver-stain was shown in Fig. S1. DNA-to-protein ratios of the conjugates were estimated by UV-VIS absorption and typically fell in the range of 2-to-1. Protein-DNA conjugates were stored at 4 °C for short-term usage or aliquoted for long-term storage at -80 °C.

DNA sequences.

All DNA sequences used in this study are provided in supplementary Table S1.

Clinical samples.

Oral fluids sample were collected using Orasure oral specimen collection device following manufacture's instructions. Briefly, oral fluid collection pad was inserted between cheek and gums for 5-7 min. Thereafter, the collection pad was stored in the collection tube containing storage buffer. The oral fluid

specimen was then transferred to Alameda County Public Health lab at room temperature. Once received, oral fluid specimens were eluted by centrifugation at 800 g for 15 min. Each oral fluid specimen contains 0.7-1.5 mL of liquids. HIV status were determined by a two-tier algorithm. Avioq HIV-1 Microelisa were used as a first tier assay, where positive samples were confirmed by Orasure western blots. All oral fluids samples used in this study were de-identified remnant samples from HIV screening program at Alameda County, and had been stored at -20 °C. The study protocol (ID: 36631) was approved by Stanford University institutional review board.

Singleplex ADAP.

Paired protein-DNA conjugates (1 femtomole) were suspended in 2 µL of buffer C (2% BSA, 0.2% Triton X-100, 8 mM EDTA, 100 µM of competition DNA, 1 mg/mL goat IgG in PBS). A 1 µL of analyte was added to the conjugates and then incubated at 37 °C for 30 min. A 117 µL of ligation mix (20 mM Tris, 50 mM KCl, 20 mM MgCl2, 20 mM DTT, 25 µM NAD, 0.025 U/µl ligase, 100 nM connector, 0.01% BSA, pH=7.5) was added and incubated at 30 °C for 15 min. A 25 µL of the solution was added to 25 µL 2x PCR Mix with 10 nM primers and then amplified by PCR (95 °C for 10 min, 95 °C for 15 sec, 56 °C for 30 sec, 12 cycles). The PCR reaction was then diluted 1:20 in H2O. A 8.5 µL of the diluted PCR samples was added to 10 µL 2x qPCR Master Mix with 1.5 µL primers (final primer concentration 690 nM). SYBR green-based qPCR was performed on a Bio-Rad CFX96 real-time PCR detection system (95 °C for 10 min, 95 °C for 30 sec, 56 °C for 1 min, 40 cycles).

The choice of 1 µL sample volume was based on the observation that using larger volumes could lead to increased background in some clinical samples. In addition, there was the practical issue that volumes below 1µL were difficult to replicate.

Importantly, to correct potential drift in qPCR signal across different experiments, a blank sample was always run concurrently to the actual sample of interest. Briefly, in contrast to add real analyte, 1 µL of PBS buffer was added as blank control. Rest of the procedure then followed the protocol outlined above.

The ADAP assay readout ΔCt was defined as the Ct value of blank minus Ct value of actual samples (Figure S3). The value of ΔCt was proportional to the initial amplicon concentrations in the PCR plate well. This amplicon concentration was also proportional to the amount of target antibodies present in the samples. (For each curve, the PCR cycle number with fluorescence value

corresponding to the chosen threshold value was defined as the cycle threshold Ct).

Multiplex ADAP.

The protocol was similar to singleplex ADAP analysis with minor modifications. Briefly, 1 femtomole of all protein-DNA conjugates was suspended in 2 µL of buffer C. Then, analyte and ligation mix was added and incubated sequentially as described above. Then, 25 µL of ligated solution was aliquoted into different wells of PCR tubes that each contained PCR master mix and one primer pairs. The pre-amplified products were then quantified by different primer pairs in a 96-well qPCR plate. Finally, ΔCt for each DNA amplicon/primers was calculated and therefore allowed multiplex quantification of multiple antibody targets from a single sample.

Analysis of purified HIV-patient antibodies.

Purified patient-derived human HIV antibodies against p24, gp41 and gp160 (ImmunoDx) were serially ten-fold diluted in buffer C and subjected to either ADAP analysis in our laboratory or clinical EIA testing (Avioq microelisa) at the Alameda County Public Health Laboratory. Each sample was run in triplicate. The dilution curve was modeled by 4 parameter logistic fit (29). The limit of detection was then defined as the average ΔCt value of the buffer C only blank plus 3 standard deviations of the blank (30). In this work, we measured buffer C only blank in triplicate to derive the standard deviations. The limit of detection was calculated relative to the blank (30).

Analysis of clinical HIV oral fluid samples.

The remnant HIV OF samples were obtained from Alameda County Public Health Lab. The 22 HIV-positive oral fluids showed EIA signals above the cutoff and showed two or more reactive bands on western blot. These positive samples were carefully selected to display a wide range EIA signal intensities to challenge ADAP's assay performance (signal-to-cutoff S/C ratio ranges from 1.7-6.7). The 22 HIV-negative oral fluid samples showed signal below the EIA cutoff (S/C ratio ranges from 0.1-0.3). The 8 indeterminate HIV samples showed EIA signal close to the cutoff (S/C ratio ranges from 0.6-0.9). Furthermore, these samples showed one weakly reactive band in western blot analysis (Orasure), and thus rendered them HIV-"indeterminate". The Alameda County Public Health Laboratory obtained a follow-up finger prick for one indeterminate sample donor and confirmed the patient HIV infected.

In singleplex ADAP analysis, p24-, gp41-, gp120- and gp160-DNA

conjugates were used separately to detect antibody reactivity in oral fluid. In a multiplex experiment, p24-, gp41- and gp120-DNA conjugates that contained unique DNA barcodes were used simultaneously to profile anti-HIV antibody response in oral fluid samples. Gp160 was not employed in multiplex experiment because gp41 and gp120 display the entire amino acid sequence of gp160. We thus did not foresee additional benefit of including gp160.

Data analysis.

In the ADAP to EIA correlation analysis, the ADAP signals were the geometric sum of ΔCt value of p24, gp41 and gp120. The sum signals were then correlated to the logarithm of EIA signals. The use of logarithm was necessary as ΔCt is a logarithmic parameter (31). (For instance, consider a sample of ΔCt value 2 and another sample of ΔCt of 4, their amplicon quantities differ by 4 fold (24/22) rather than 2 fold.)

SUPPLEMENTARY MATERIALS

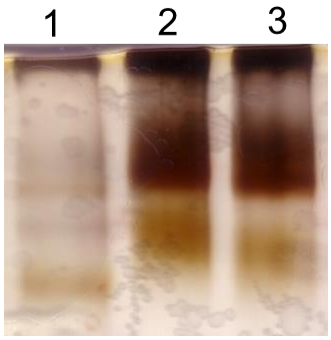

Figure S1. Representative SDS-PAGE and silver stain for viral antigen-DNA conjugation. Lane 1, unconjugated gp120. Lane 2 and 3, conjugated gp120 with DNA. A clear mass shift can be observed after conjugation with DNA. The unconjugated gp120 protein existed as monomer, dimer and trimer. The lowest band in Lane 2 and Lane 3 corresponded to DNA conjugated gp120 monomer, whereas the upper dark band in Lane 2 and Lane 3 corresponded to DNA conjugated gp120 dimer and trimer.

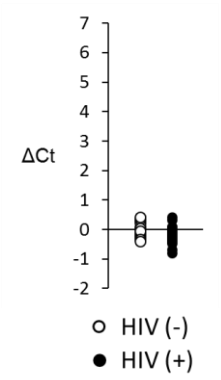

Figure S2. ADAP analysis of clinical oral fluid with GFP-DNA conjugates. To re-affirm there was no intrinsic difference between HIV positive and HIV negative oral fluid, we used GFP-DNA conjugates as negative control. Since human oral fluid should not contain anti-GFP antibodies, we expected no signal to be generated from both sample sets. Satisfyingly, we did not observe any difference in signal intensity between HIV positive and HIV negative fluids. These results confirmed that signals observed following ADAP analysis was indeed specific to viral antigen-DNA conjugates.

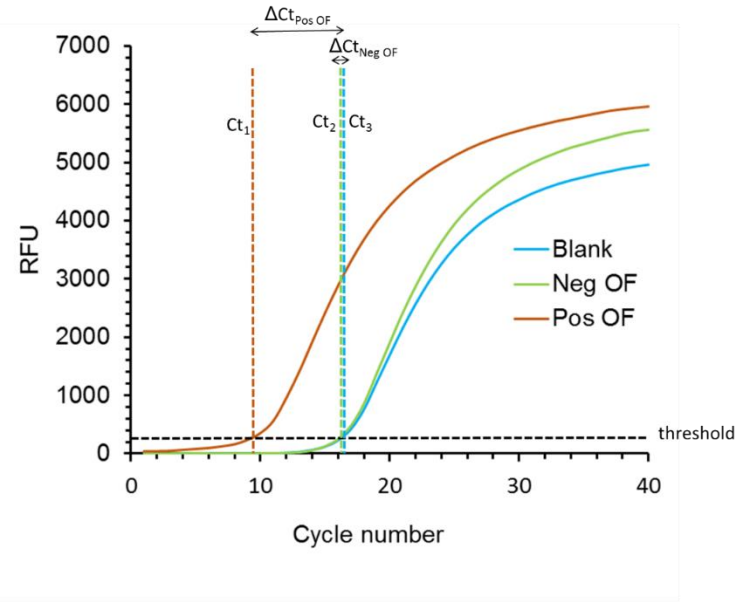

Figure S3. Representative real-time quantitative PCR (qPCR) curves for ADAP experiments. In a standard SYBR qPCR experiment, fluorescent values (RFU, y-axis) would gradually increase as PCR cycling went on (Cycle number, x-axis). For instance, here we illustrated representative qPCR curves for HIV oral fluid (OF) using p24-DNA conjugates. The Ct value of qPCR was defined as the cycle number where fluorescent readout of the sample equaled a defined threshold fluorescent value (black horizontal dash line). The Ct value of HIV

positive oral fluid (abbreviated as Pos OF) was 9.29 (Ct1, brown vertical dash line), whereas Ct value of HIV negative oral fluid (abbreviated as Neg OF) and blank control were 16.09 (Ct2, green vertical dash line) and 16.31 (Ct3, blue vertical dash line) respectively. The ΔCt of an ADAP experiment was defined as the Ct value difference between a sample and a blank control. Therefore, the ΔCt for Pos OF will be 7.02 (16.31-9.29), and ΔCt for Neg OF will be 0.22 (16.31-16.09). A larger ΔCt indicated that the sample contained higher amount of PCR amplicons, which then reflected the presence of higher amount of antibodies.

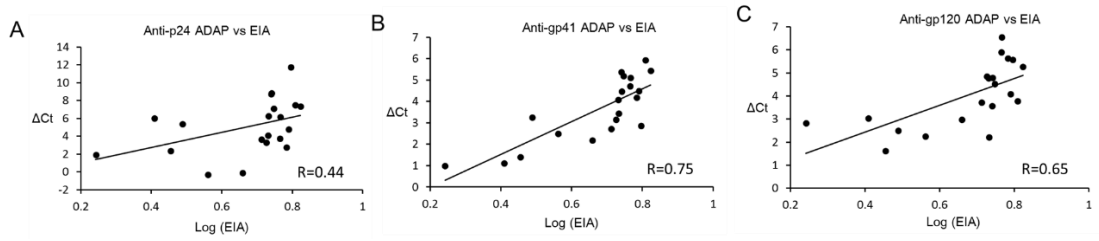

Figure S4. Correlations of individual HIV component ADAP assay vs EIA. The same oral fluids in Fig 3C were re-analyzed to investigate correlations between two methods. A, Signal intensities measured by p24-DNA conjugates in ADAP vs EIA. B, Signal intensities measured by gp41-DNA conjugates in ADAP vs EIA. C, Signal intensities measured by gp120-DNA conjugates in ADAP vs EIA. (EIA used whole HIV viral lysates as antigens).

Singleplex	Sequence A	Sequence B	Forward primer	Reverse primer
p24,gp41,gp120, gp160	thiol-CAGGTAGTAGTACGTCTGTTTCACGATGAGACTGGATGAA	phos-TCACGGTAGCATAAGGTGCAAGATAATACTCTCGCAGCAC-thiol	CAGGTAGTAGTACGTCTGTT	GTGCTGCGAGAGTATTATCT
Multiplex	**Sequence A**	**Sequence B**	**Forward primer**	**Reverse primer**
p24	thiol-CAGGTAGTAGTACGTCTGTTTCACGATGAGACTGGATGAA	phos-TCACGGTAGCATAAGGTGCAAGATAATACTCTCGCAGCAC-thiol	CAGGTAGTAGTACGTCTGTT	GTGCTGCGAGAGTATTATCT
gp41	thiol-GGCCTCCTCCAATTAAAGAATCACGATGAGACTGGATGAA	phos-TCACGGTAGCATAAGGTGCAGTACCCAAATAACGGTTCAC-thiol	GGCCTCCTCCAATTAAAGAA	GTGAACCGTTATTTGGGTAC
gp120	thiol-GGATCACTCCAACTAGACTATCACGATGAGACTGGATGAA	phos-TCACGGTAGCATAAGGTGCAGTTATATCTGCCACTGTCAC-thiol	GGATCACTCCAACTAGACTA	GTGACAGTGGCAGATATAAC
Connector	CTACCGTGATTCATCCAG			
Competition Oligo	TCGTGGAACTATCTAGCGGTGTACGTGAGTGGGCATGTAGCAAGAGGGTCATCATTCGAA			

Table S1. DNA sequences. In singleplex experiment, all viral antigens were conjugated to the same set of DNA sequences. In multiplex experiment, each viral antigen were conjugated to a specific pair of DNA barcodes. Sequence A was 5' thiolated to enable conjugation. Sequence B was 3' thiolated to enable conjugation and 5' phosphorylated to enable ligation. All DNA barcodes shared the same connector sequence (21). The competition oligo was added in excess to prevent nonspecific binding to protein-DNA conjugates.

Panel member	Stage	ADAP			Bio-rad Genetic Systems HIV1/2 plus O EIA	Orasure OraQuick ADVANCE HIV-1/2 Antibody Test
		gp41	p24	gp120		
5	I	-0.23778	-0.29556	-0.5	0.05	0
6	I	0.302222	-0.09556	0.06	0.09	0
7	I	0.222222	0.184444	0.07	0.05	0
8	I	2.102222	-0.16556	0.15	0.03	0
9	II	2.172222	-0.16556	-0.13	0.04	0
10	II	2.502222	1.464444	-0.39	0.04	0
11	II	1.282222	-0.16556	1.28	0.03	0
12	II	-0.48778	-0.41556	-0.51	0.04	0
13	III	5.572222	1.454444	0.45	3.4	0
14	III	5.592222	0.314444	0.53	1.8	0
15	III	1.862222	-0.11556	-0.06	1.2	0
16	III	2.548333	-0.8625	0.98	2	0
17	IV	2.778333	3.4275	2.1	3.5	weak positive
18	IV	4.058333	-0.5825	3.81	3.6	weak positive
19	IV	2.588333	-0.1525	0.2	3.6	0
20	IV	3.518333	4.4875	3.25	3.6	0
21	V	4.618333	11.3775	4.96	3.6	positive
22	V	4.008333	2.2675	4.51	3.7	positive
23	V	4.378333	10.2275	4.59	3.7	strong positive

Table S2. ADAP analysis of IgM positive HIV serum. Early infected HIV patient serum sample panel was purchased from SeraCare (#0800-0297). These samples had been analyzed extensively by various HIV assays in reference laboratory, including 3rd-generation HIV antibody assay and rapid HIV antibody assay. In particular, panel member 13 to 16 only had detectable HIV signals by 3rd-generation HIV assay (Bio-rad, capable of detecting IgM anti-HIV) but not by HIV rapid assay (Orasure, not capable of detecting IgM anti-HIV), indicating these samples contained IgM anti-HIV antibodies. Satisfyingly, ADAP HIV assays indeed showed detectable HIV antibodies signals for these samples, affirming ADAP's capabilities to detect antibodies of IgM class. Furthermore, panel member 8-10 had detectable HIV antibodies signals by ADAP but not by either 3rd generation or rapid HIV antibody assays. These results implied higher sensitivity of ADAP might shorten HIV detection window period as compared to

other HIV antibodies assays. (The assay cutoffs for ADAP HIV serum assays were defined by 12 HIV negative control serum samples purchased from RDL Inc. The cutoffs were 3 standard deviation plus average signals of negative control serum, which corresponds to 99% assay specificity.) *Red bold font for positive signals.

REFERENCE.

1. Bayer R, Oppenheimer GM (2013) Routine HIV testing, public health, and the USPSTF-an end to the debate. N Engl J Med 368:881-884.
2. Hollingsworth TD, Anderson RM, Fraser C (2008) HIV-1 transmission, by stage of infection. J Infect Dis 198:687-693.
3. Powers KA, et al. (2011) The role of acute and early HIV infection in the spread of HIV and implications for transmission prevention strategies in Lilongwe, Malawi: a modelling study. Lancet 378:256-268.
4. Carballo-Diéguez A, Frasca T, Dolezal C, Balan I (2012) Will gay and bisexually active men at high risk of infection use over-the-counter rapid HIV tests to screen sexual partners? J Sex Res 49:379-387.
5. Stekler JD, et al. (2013) Relative accuracy of serum, whole blood, and oral fluid HIV tests among Seattle men who have sex with men. J Clin Virol 58:e119-122.
6. Luo W, et al. (2013) Comparison of HIV oral fluid and plasma antibody results during early infection in a longitudinal Nigerian cohort. J Clin Virol. 58:e113-118.
7. Pilcher CD, et al. (2013) Performance of rapid point-of-care and laboratory tests for acute and established HIV infection in San Francisco. PLoS One 8:e80629.
8. Merson MH, O'Malley J, Serwadda D, Apisuk C (2008) The history and challenge of HIV prevention. Lancet 372:475-488.
9. Beckwith CG, et al. (2011) An evaluation of a routine opt-out rapid HIV testing program in a Rhode Island jail. AIDS Educ Prev 23:96-109.
10. Hodinka RL, Nagashunmugam T, Malamud D (1998) Detection of human immunodeficiency virus antibodies in oral fluids. Clin Diagn Lab Immunol 5:419-426.
11. Sherman GG, Jones SA (2005) Oral fluid human immunodeficiency virus tests: improved access to diagnosis for infants in poorly resourced prevention of mother to child transmission programs. Pediatr Infect Dis J 24:253-256.
12. Kowalczyk Mullins TL, Braverman PK, Dorn LD, Kollar LM, Kahn JA (2011) Adolescent preferences for human immunodeficiency virus testing

methods and impact of rapid tests on receipt of results. J Adolesc Health. 46:162-168.
13. Schramm W, Angulo GB, Torres PC, Burgess-Cassler A (1999) A simple saliva-based test for detecting antibodies to human immunodeficiency virus. Clin Diagn Lab Immunol. 6(4):577-80.
14. Tourinho RS, de Almeida AJ, Amado LA, Villar LM, Castro AR, de Paula VS (2012) Could oral fluid be used to evaluate anti-hepatitis A virus status in individuals living in difficult-to-access areas? Vaccine 30(45):6421-6.
15. Page-Shafer K, Sweet S, Kassaye S, Ssali C (2006) Saliva, breast milk, and mucosal fluids in HIV transmission Adv Dent Res 19:152-157.
16. Corstjens PL, Abrams WR, Malamud D (2012) Detecting viruses by using salivary diagnostics. J Am Dent Assoc 143:12S-8S.
17. Balamane M, et al. (2010) Detection of HIV-1 in saliva: implications for case-identification, clinical monitoring and surveillance for drug resistance. Open Virol J 4:88-93.
18. U.S. Food and Drug Administration. OraQuick In-Home HIV Test: Summary of Safety and Effectiveness. [Accessed December 17, 2012]; Available at: http://www.fda.gov/downloads/BiologicsBloodVaccines/BloodBloodProducts/ApprovedProducts/PremarketApprovalsPMAs/UCM312534.pdf.
19. Taylor D, et al. (2015) Probability of a false-negative HIV antibody test result during the window period: a tool for pre- and post-test counselling. Int J STD AIDS. 26:215-224.
20. Louie B, Lei J, Liska S, Dowling T, Pandori MW (2009) Assessment of sensitivity and specificity of first, second, and third generation EIA for the detection of antibodies to HIV-1 in oral fluid. J Virol Methods 159:119-121.
21. Tsai CT, Robinson PV, Spencer CA, Bertozzi CR (2016) Ultrasensitive antibody detection by agglutination-PCR (ADAP). ACS Cent Sci 2:139-147.
22. Buttò S, Suligoi B, Fanales-Belasio E, Raimondo M (2010) Laboratory diagnostics for HIV infection. Ann Ist Super Sanita 46:24-33.
23. Fredriksson S, Dixon W, Ji H, Koong AC, Mindrinos M, Davis RW (2007) Multiplexed protein detection by proximity ligation for cancer biomarker validation. Nat Methods. 4:327-329.
24. Cornett JK, Kirn TJ (2013) Laboratory diagnosis of HIV in adults: a review of current methods. Clin Infect Dis 57(5):712-718.
25. Chang L, et al. (2013) Simple diffusion-constrained immunoassay for p24 protein with the sensitivity of nucleic acid amplification for detecting acute HIV infection. J Virol Methods. 188(1-2):153-60.

26. US Food & Drug Administration. HIV/AIDS Historical Time Line 1981-1990. https://www.fda.gov/forpatients/illness/hivaids/history/ucm151074.htm
27. Wilkinson E, Engelbrecht S, de Oliveira T (2015) History and origin of the HIV-1 subtype C epidemic in South Africa and the greater southern African region. Sci Rep 5:16897.
28. Lemey P, et al. (2003) Tracing the origin and history of the HIV-2 epidemic. Proc Natl Acad Sci U S A 100(11):6588-6592
29. Findlay JWA, Dillard RF (2007) Appropriate calibration curve fitting in ligand binding assays. AAPS J 9:260-267.
30. Armbruster DA, Pry T (2008) Limit of blank, limit of detection and limit of quantitation. Clin. Biochem Rev 29:S49-S52.
31. Niemeyer C, Adler M, Wacker R (2007) Detecting antigens by quantitative immuno-PCR. Nat. Protoc. 2:1918-1930.

Chapter 4
Isotype specific agglutination-PCR (ISAP) for detection of selective antibody isotypes

Chapter 4. Isotype specific agglutination-PCR (ISAP) for detection of selective antibody isotypes*

In this chapter, I am going to describe a second generation of PCR-based immunoassay that would complement previously described ADAP technology. The new assay termed ISAP allows specific quantification of antibody of selective isotypes even in the presence of large amount of background antibodies. This assay would allow researchers and clinicians to zoom in on specific antibody isotype responses of interest. I will describe development of ISAP toward allergy applications.

*Kaori Mukai, PhD and Peter Robinson contributes significantly to results described in this chapter. The content of this chapter has been published at JACI, 2017.

Isotype-Specific Agglutination-PCR (ISAP): a sensitive and multiplex method for measuring allergen-specific IgE, The Journal of allergy and clinical immunology, 2017

Introduction.

Component-resolved diagnostics (CRD) are a rapidly-growing class of in-vitro tests for evaluating individuals thought to have allergic diseases. In contrast to using whole-allergen extracts, CRD employs individual, molecularly pure allergen components to measure allergen-specific IgE (sIgE), thereby helping to assess the risk of allergy to such allergens with improved accuracy1. For example, the presence of sIgE against certain peanut components (e.g., Ara h 1, Ara h 2 and Ara h 3) indicates a higher risk for anaphylaxis than does anti-Ara h 8 sIgE (which can reflect cross-reactivity with birch pollen)1. While ELISA-based CRD tests may lack analytical sensitivity, the alternative more sensitive assays currently employed clinically (e.g., ImmunoCAP) are not multiplexible and may omit certain critical allergens2. These problems can be mitigated by collecting more blood for additional tests. However, this approach can be problematic when studying small animals or testing young children.

Here we report Isotype-Specific Agglutination-PCR (ISAP), a highly sensitive and multiplexible approach for measuring allergen-specific immunoglobulins (Igs) in 1 μL of sample (Fig 1, A). ISAP employs chemically-synthesized allergen-DNA and secondary antibody-DNA conjugates (see Fig E1 in this article's Online Repository at www.jacionline.org). Each DNA

conjugate bears either the 5' or 3' portion of a split DNA barcode (Fig 1, A). Upon binding to the target Ig in the sample, the allergen-DNA and secondary antibody-DNA conjugates are agglutinated into close proximity. The addition of a short complementary bridge oligo and DNA ligase reunites the two halves of the barcode to create a full-length DNA amplicon, which can then be quantified by qPCR. The amount of the amplicon directly reflects the quantity of analyte within the sample. Importantly, in the absence of the specified allergen-specific Ig, the two DNA conjugates will neither ligate nor amplify by PCR. By requiring the presence of the analyte to generate signal, this "turn-on" mechanism circumvents the washing or DNA purification steps needed to remove unbound secondary reporters in other formats such as immuno-PCR3,4. In principle, these features allow ISAP to represent a CRD assay with enhanced sensitivity, multiplex capability, and an operationally simple workflow.

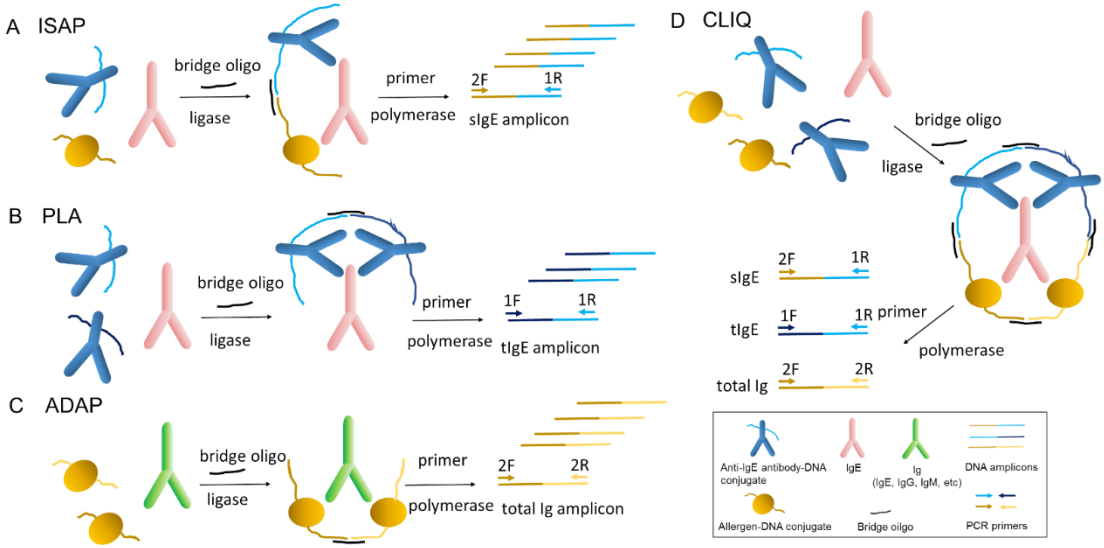

Figure 1. Principle scheme of PCR-based antibody quantification methods. (A) ISAP for quantification of sIgE. Samples containing sIgE are first incubated with allergen-DNA and antibody-DNA (in this case, anti-IgE antibody-DNA) conjugates. Upon formation of immune complexes consisting of sIgE, allergen-DNA and anti-IgE-DNA, the DNA components of the conjugates are brought into close proximity, and the addition of a short bridge oligo and DNA ligase joins the two halves of DNA into a full length amplicon. Real-time qPCR is then used to quantify the abundance of the ligated DNA amplicons, which reflects the level of sIgE in the sample. (B) PLA for quantification of total IgE (tIgE). Samples are incubated with two anti-IgE-DNA conjugates that each bear half of a full-length DNA amplicon. (C) ADAP for quantification of all anti-allergen immunoglobulins (IgE, IgG, IgM, etc.). This procedure is performed as before,

but with two allergen-DNA conjugates. (D) Integration of ISAP, PLA and ADAP into a single assay, termed CLIQ. The sample is incubated with two allergen-DNA and two anti-IgE-DNA conjugates followed by ligation. The reconstituted DNA amplicons can be interrogated independently by dedicated primer pairs in the different wells of a 96- or 384-well plate.

Results and Discussion

Benchmark ISAP using purified antibodies.

To establish proof-of-concept for the detection of allergen-specific IgE (sIgE), we prepared a dilution series of: 1) anti-OVA sIgE, 2) anti-OVA sIgG and 3) total IgE (control). The three samples were then analyzed with an ISAP assay designed to detect anti-OVA sIgE. As expected, concentration-dependent signal arose only for the sample containing anti-OVA sIgE (Fig 2, A). Next, we performed a head-to-head comparison of ISAP with a standard ELISA, which showed a markedly (~800-fold) increased analytical sensitivity of ISAP compared to ELISA (Fig 2, B).

In addition to sIgE, total IgE and total anti-allergen sIg levels (of all Ig classes) are also of interest in characterizing allergic responses. To create an assay capable of measuring these parameters, we integrated ISAP with two other PCR-based methods: the Proximity Ligation Assay (PLA)5 and Antibody Detection by Agglutination-PCR (ADAP)6 (Fig 1, B and C). PLA employs two secondary antibody-DNA conjugates to detect total IgE (tIgE) whereas ADAP uses two allergen-DNA conjugates to detect all allergen-specific Igs (e.g., IgE, IgG, IgM). The integrated assay, termed CLIQ (Comprehensive Ligation-based Immunoglobulin Quantification), converts sIgE, tIgE and all sIgs of any isotypes into distinct DNA amplicons that can be independently interrogated with unique primer pairs (Fig 1, D).

Benchmark CLIQ using purified antibodies.

To validate this concept, we re-analyzed the anti-OVA sIgE, anti-OVA sIgG and total IgE (control) dilution series with CLIQ (see Fig E2 in this article's Online Repository at www.jacionline.org). For instance, Fig E2, A shows that both the PLA (which measures total IgE, solid squares) and the ISAP (which measures sIgE, open triangles) portions of CLIQ lacked signals when used to assess anti-OVA sIgG; only the ADAP portion of CLIQ (which measures total anti-OVA sIgs, solid circles) shows concentration-dependent signals. The data in Fig E2 indicate that each of the three PCR-based methods selectively detected its specified target in an integrated assay without cross-reactivity.

Validate ISAP using mouse models.

Next, we sensitized mice with OVA7 and analyzed their antibody responses using CLIQ. CLIQ demonstrated elevations in serum and blood levels of tIgE and total anti-OVA sIg at d7 and sIgE at d14 in OVA-sensitized mice, but not in PBS-treated control mice (see Fig E3, A and C, and Fig E4). ELISA also detected an elevation in serum sIgE at d14 in the same OVA-sensitized mice (see Fig E3, B). These results demonstrate substantial equivalence between the CLIQ and ELISA methods in this setting, in which strong sIgE responses are induced.

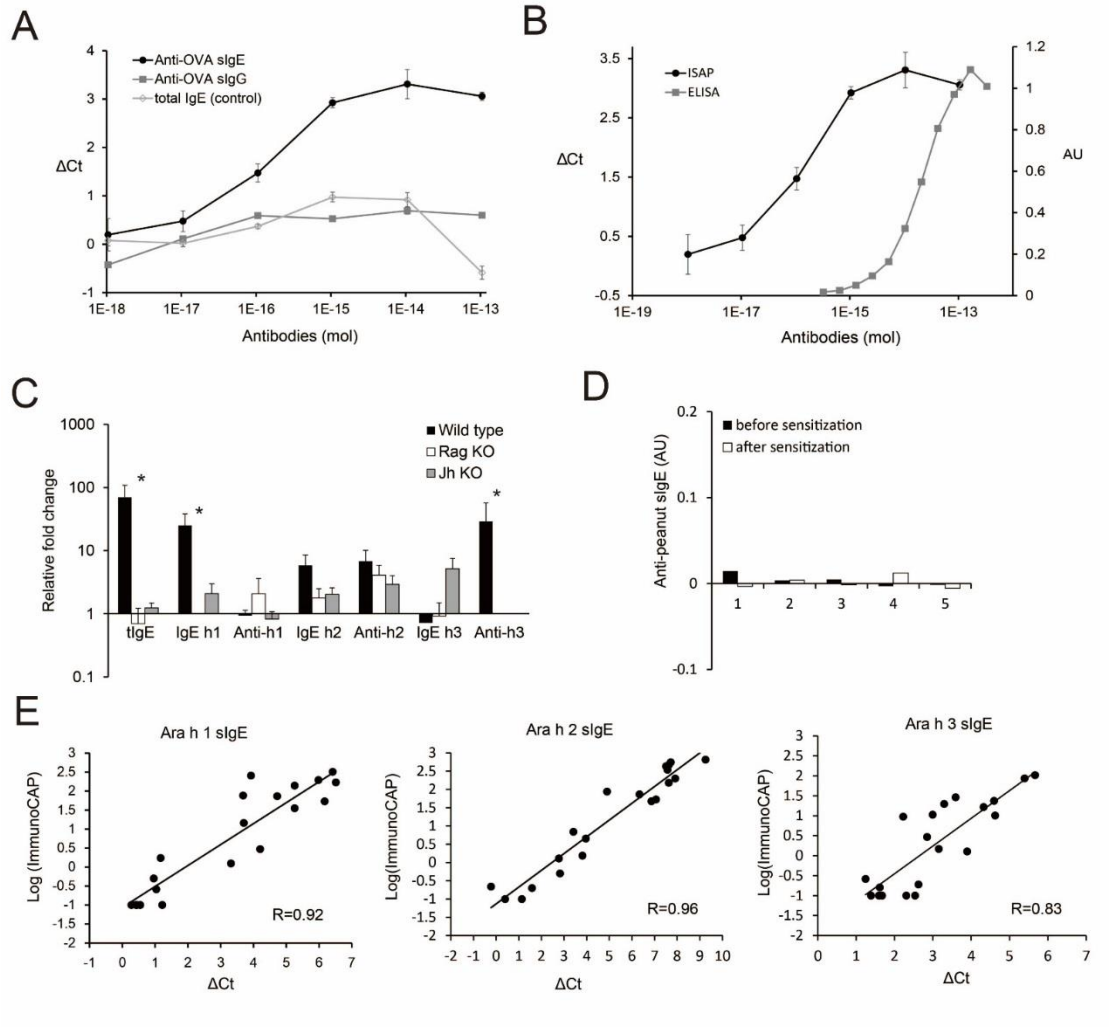

Figure 2. Multiplex and sensitive detection of allergy-related immunoglobulins by PCR. (A) Serially-diluted anti-OVA sIgE, anti-OVA sIgG and total IgE (control) analyzed with ISAP (ΔCt [Delta Cycle threshold], a standard way to report qPCR signal=Ct value of buffer-only control minus that of sample). (B) Aliquots of the same anti-OVA sIgE dilution series assayed by ISAP (ΔCt) and ELISA

(AU=arbitrary units). (C) CLIQ profiles of immunoglobulin responses to peanut sensitization in BALB/c wild type mice, BALB/c-Rag-/- (Rag KO) mice and BALB/c-Jh-/- (Jh KO) mice (n=5/group) sensitized to peanut epicutaneously. CLIQ results are expressed as the relative fold change (value after sensitization divided by value before sensitization) (* $P < .05$ for values before vs. after sensitization). The h1, h2 and h3 labels in the x-axis refer to Ara h1, Ara h2 and Ara h3, respectively. (D) ELISA analysis of sera from the same 5 BALB/c mice analyzed by ISAP in C. No statistically significant differences in levels of anti-peanut sIgE were observed by ELISA before vs. after sensitization. (E) Correlation of ISAP and ImmunoCAP results ($R=0.83$-0.96, $P < .05$). 1 μL each of 20 baseline (pre oral immunotherapy) plasma specimens from participants in the POISED trial analyzed by ISAP (x-axis) vs. ImmunoCAP (y-axis).

Validate ISAP using peanut allergic mouse models.

To probe the sensitivity of CLIQ in settings with low levels of serum sIgE, we sensitized mice epicutaneously with peanut oil. The sensitized mice were later challenged with peanut extract to attempt to induce anaphylaxis. Despite the strong systemic reaction to peanut challenge (see Fig E5 in this article's Online Repository at www.jacionline.org), peanut sIgE was undetectable by ELISA (Fig 2, D and Fig E6). However, when we assayed serum from these mice with CLIQ (using multiple peanut components as antigens: Ara h 1, Ara h 2 and Ara h 3), CLIQ, but not ELISA, detected increases in tIgE and Ara h 1 sIgE after peanut oil sensitization in BALB/c or C57BL/6 mice (Fig 2, C and see Figs E7 and E8 in this article's Online Repository at www.jacionline.org). By contrast, CLIQ did not detect such changes in antibody-deficient Jh-/- and Rag-/- mice after we attempted to induce peanut sensitization8 (Fig 2, C). These results show that the enhanced analytical sensitivity of CLIQ can detect potentially disease-relevant levels of sIgE which may be undetectable by traditional means like ELISA.

Validate ISAP using peanut allergy clinical trial samples.

Finally, we employed CLIQ to analyze plasma obtained from 20 peanut-allergic subjects upon their enrollment into the IRB-approved POISED trial (ClinicalTrials.gov Identifier: NCT02103270)9. CLIQ results displayed substantial positive correlations with ImmunoCAP data from the same specimens (Fig 2, E and see Figs E9, E10 and E11 in this article's Online Repository at www.jacionline.org).

It is important to emphasize that no assay for sIgE can be used, in isolation,

to establish the diagnosis of a clinically relevant allergy. However, such testing, if used appropriately, can identify those who have been sensitized to specific allergens or their components and therefore can confirm that these individuals are potentially at risk for exhibiting sIgE-associated clinical allergies. Although it is not possible to fully prevent the misuse of any diagnostic assay, and this is a particular concern with highly sensitive assays, our data suggest that, as with the ImmunoCAP assay, appropriate selection of the assay cutoff value will permit the CLIQ assay to be used to identify potentially clinically relevant levels of sIgE against allergen components.

In summary, ISAP is a sensitive and specific method for multiplex detection of isotype-specific sIgE against specific allergen components in very small (1 µL) sample volumes. Integration of ISAP with PLA and ADAP to create the CLIQ assay greatly expands the information which can be obtained in a single assay. We envision that the much lower sample consumption and improved sensitivity of this assay will prove useful for allergy research and diagnostics, and for the management of allergy patients.

METHODS

Materials and Reagents.

Chemicals (including KCl, MgCl2, Tris, EDTA, NAD, Triton X-100 and bovine serum albumin) were purchased from Sigma Aldrich (St. Louis, MO) or DMSO, DTT, sulfo-SMCC and dNTP from Life technologies (Carlsbad, CA). All oligonucleotides were manufactured by Integrated DNA Technologies (abbreviated as IDT, Redwood City, CA). The specific sequences for all oligonucleotides are provided in the DNA sequence table immediately below. Anti-ovalbumin IgE was from AbD Serotec (#MCA2259, Hercules, CA), IgE isotype control (also referred to as total IgE control [tIgE]) was from Biolegend (#401701, San Diego, CA) and anti-ovalbumin IgG was from Abcam (ab17293, Cambridge, United Kingdom). OVA protein was from Life Technologies (#77120) and Ara h1 (#LTN-AH1-1), Ara h2 (#RP-AH2-1) and Ara h3 (#NA-AH3-1) were from Indoor Biotechnologies (Charlottesville, VA). Anti-mouse IgE antibody was from Abcam (#ab19967), anti-human IgE antibody was from AbD Serotec (#STAR147), DNA ligase was from EpiCentre (#A8101, Madison, WI) and DNA polymerase (#10966018) and SYBR qPCR 2X master mix (#4385610) were from Thermo Fisher (Waltham, MA). DNA sequences with an A in their name have a 5’ thiol-group (5’-thiol modifier C6 S-S) to enable conjugation to proteins, whereas DNA sequences with a B in their name have 5’ phosphorylation to enable ligation and a 3’ thiol-group (3'-thiol modifier C3 S-S) to enable

conjugation. DNA sequences and primers were optimized to minimize formation of secondary structures and primer dimers while maximizing amplification efficiency.

Analysis of human plasma.

Plasma samples from patients with peanut allergy were obtained as part of their enrollment into an institutional review board-approved clinical trial of oral immunotherapy (OIT) in children and adults with peanut allergy (POISED; ClinicalTrials.gov Identifier: NCT02103270). Peanut allergy was defined as having a reaction to a double-blind, placebo-controlled food challenge to peanut (with reactions elicited with <=500 mg of peanut protein) and a positive skin prick test response to peanut (wheal >=5 mm).

OVA sensitization.

Sensitization of mice was achieved by administration of OVA with alum. The protocol was performed as described in 1, with minor modifications. Briefly, mice (n=5/group) were immunized intraperitoneally with 100 µg OVA (Grade V; Sigma-Aldrich, St Louis, MO), 100 ng of B pertussis toxin (List Biologicals, Campbell, CA), and 50 µL Imject Alum (Thermo Scientific, Waltham, MA) in PBS in a total volume of 100 µL on days 0 and 14. Control mice (n=5) were inoculated similarly with 100 µL of a solution containing 100 ng of B pertussis toxin and 50 µL Imject Alum in PBS, but without OVA. Serum and whole blood samples were collected via retro-orbital bleeding on days 0, 7, 14, and 21. All serum samples were stored at -80°C until used. Whole blood samples were diluted 1:1 in 10 mM EDTA and 1X PBS right after collection to prevent clotting. Whole blood samples were stored at -80°C until used.

Sensitization with peanut oil and intraperitoneal challenge with peanut protein. The abdominal skin of BALB/c wild type mice, C57BL/6 wild type mice, BALB/c-Jh-/- mice and BALB/c-RAG-/- mice (all n=5/group) was shaved and then depilated with Veet (Reckitt Benckiser, Slough, United Kingdom), followed by washing with PBS, and the mice then were sensitized once a week with 200 µL of peanut oil (#570600, Golden Peanut Company, Dawson, Georgia) for 6 weeks. Per the manufacturer, the peanut oil is crude oil without any filtration or refinement, and Jablonski, et al. confirmed the presence of peanut protein (approx. 400 ppm) in this oil using colorimetric assays 2. After application, each mouse was gently held by the investigator for 1 min for the peanut oil to be absorbed, and then 3-5 mice treated in this way were housed in the same cage. BALB/c and C57BL/6 mice were then challenged i.p. with 5 mg of peanut

protein (extracted from defatted peanut flour as previously described (Byrd Mill, Ashland, Virginia) 3 administered in 300 µL of PBS, or received PBS alone as a control. Rectal measurements of body temperature were performed immediately before (time 0) and at different time points for up to 60 minutes after challenge, as described above. Serum samples (stored at -80°C until used) were collected on day 0 via retro-orbital bleeding and on day 42 via cardiac puncture after sacrificing the mice by inhalation of CO2.

ELISA analysis.

The ELISA to measure specific IgE (sIgE) was performed as described in 1 with minor modifications. Briefly, OVA was deposited on ELISA plates to capture and detect anti-OVA IgE in samples of purified IgE or in serum from OVA-sensitized mice. The amount of surface-bound IgE was quantified by detecting absorbance after treatment with biotinylated secondary anti-mouse IgE and streptavidin horseradish peroxidase conjugate (SA-HRP). The SA-HRP reacts with its substrate TMB (3,3',5,5'-Tetramethylbenzidine, Thermo Fisher) to yield a colorimetric reaction that can be quantified by a plate reader. For the detection of peanut-specific IgE, whole peanut extract (#F171, Greer Laboratories, Lenoir, NC) was coated on ELISA plates and anti-peanut IgE was detected as described above. This ELISA method should detect all peanut specific IgE. To further measure Ara h 1 sIgE, we followed the protocol of Smit, et al., and Van Wijk, et al. as detailed in 4, 5. Briefly, 96 well plates (Costar, Washington, D.C.) were coated with rat anti-mouse IgE (#553413, BD Biosciences, San Jose, CA) at 4°C overnight. Following blocking with 5% bovine serum albumin (Sigma-Aldrich, St. Louis, MO) in PBS for 2 h at room temperature, serum (1:8 dilution) was added for 2 h at room temperature. Digoxin (DIG) conjugated recombinant Ara h1 (10 µg/mL, #LTN-AH1-1, Indoor Biotechnologies, Charlottesville, VA) then was added and incubated for 2 h at room temperature. DIG was conjugated according to the manufacturer's instructions (#55865, digoxigenin NHS-ester, Sigma-Aldrich). After incubation for an additional 2 h at room temperature with alkaline phosphatase-conjugated anti-DIG antibody (Sigma-Aldrich), p-nitrophenylphosphate (Sigma-Aldrich) was added as a substrate and OD 405 nm was measured.

ImmunoCAP analysis.

Was performed by Phadia, Thermo Fisher (Waltham, MA).

Synthesis of allergen-DNA and antibody-DNA conjugates.

OVA was obtained from Life Technologies (#77120, Charlottesville, VA). Ara h1 (#LTN-AH1-1), Ara h2 (#RP-AH2-1) and Ara h3 (#NA-AH3-1) were purchased from Indoor Biotechnologies (Charlottesville, VA). Allergen (OVA, Ara-h1, Ara-h2 and Ara-h3)-DNA conjugates were synthesized by suspending purified or recombinant protein in Reaction Buffer (1 mg/mL protein in 55 mM sodium phosphate, 150 mM sodium chloride, 20 mM EDTA, pH 7.2). SMCC (succinimidyl 4-(N-maleimidomethyl)cyclohexane-1-carboxylate, Pierce Biotechnologies, Waltham, MA) was dissolved in anhydrous DMSO and 5 µL of a 4 mM solution was added to 50 µL of the purified or recombinant protein solution and incubated at room temperature (RT) for 2 h. Thiolated-DNA (IDT) was resuspended to 100 µM in Reaction Buffer and 3 µL was added to 50 µL of Reaction Buffer. To this solution, 4 µL of a 100 mM solution of DTT (Life Technologies) was added to reduce the oxidized thiol-DNA. The solution was then incubated at 37 °C for 1 h. 7K MWCO (molecular weight cut-off) gel microspin columns (#89882, Thermo Fisher, Waltham, MA) were equilibrated to Reaction Buffer. The excess DTT and SMCC were removed by desalting with these equilibrated columns. The thiol-DNA and allergen-SMCC solutions were then mixed and reacted overnight at 4°C and then purified by 30k MWCO filter column (Millipore, Hayward, CA). Concentrations of the conjugates were measured by BCA assay (Life Technologies). Conjugation efficiencies were determined by SDS-PAGE and silver staining as described previously 6. Representative silver-stains are provided (Fig E1). DNA-to-allergen ratios of the conjugates were estimated by UV-VIS absorption. For each protein, the median number of conjugated DNA molecules is 2.5-3. Allergen-DNA conjugates were stored at 4°C for short-term usage or aliquoted for long-term storage at -80°C. Antibody-DNA conjugates were synthesized following a similar protocol, but with minor modifications. Briefly, anti-mouse IgE antibody was from Abcam (#ab19967). Anti-human IgE antibody was purchased from AbD Serotec (#STAR147). Instead of 30K MWCO filters, 100K MWCO filter columns were used to purify the conjugates from unreacted DNA.

Isotype-specific agglutination-PCR (ISAP).

For detecting allergen-specific IgE against specific allergen components, 1 fmol of allergen-DNA conjugate and anti-IgE conjugates were suspended in 2 µL of Buffer C (2% BSA, 0.2% Triton X-100, 8 mM EDTA in PBS). To this solution, 1 µL of analyte was added and then incubated at 37°C for 30 min. After incubation, 117 µL of ligation mix (20 mM Tris, 50 mM KCl, 20 mM MgCl2, 20 mM DTT, 25 µM NAD, 0.025 U/µl ligase, bridge oligo 100 nM, 0.001% BSA,

pH=7.5) was added, and then incubated for 15 min at 30°C. After this incubation, 25 µL of the solution was added to 25 µL 2x PCR Master Mix (Thermo Fisher, Waltham, MA) with 10 nM primers and then amplified by PCR (95°C for 10 min, 56°C for 30s, 95°C for 15s, 13 cycles). The PCR reaction was then diluted 1:20 in ddH2O and 8.5 µL of the diluted PCR samples were added to 10 µL 2x SYBR qPCR Master Mix (Life Technologies) with 1.5 µL primers (final concentration 690 nM). Analysis by qPCR was performed on Bio-Rad CFX96 real-time PCR detection system. The overall process from sample input to assay completion was ~3-4 hours. Note that this method can be used to measure isotype-specific sIgE against specific allergen components; we have not attempted to produce versions for measuring sIgE against allergen extracts, which can contain a variety of different specific allergen components, often present in variable amounts in different extracts 7, 8.

Comprehensive ligation-based immunoglobulin quantification (CLIQ).

Our three-part PCR-based assay (CLIQ) is a combination of proximity ligation assay (PLA), antibody detection by agglutination-PCR (ADAP) and isotype-specific agglutination-PCR (ISAP). The combined PCR-based assay detects total IgE, total anti-allergen antibodies and allergen specific IgE (sIgE) in a single assay. The protocol is similar to ISAP with minor modifications. For the comprehensive analysis of antibodies generated in response to OVA sensitization in OVA-immunized mice, 1 fmol of OVA-2A, OVA-2B, anti-IgE-1A and anti-IgE-1B were suspended in 2 µL of Buffer C (2% BSA, 0.2% Triton X-100, 8 mM EDTA in PBS). To this solution, 1 µL of analyte was added to the conjugates and then incubated at 37°C for 30 min. Following incubation, 117 µL of ligation mix (20 mM Tris, 50 mM KCl, 20 mM MgCl2, 20 mM DTT, 25 µM NAD, 0.025 U/µl ligase, bridge oligo 100 nM, 0.001% BSA, pH=7.5) was added, and then incubated for 15 min at 30°C. Next, 25 µL of the solution was added to 25 µL 2x PCR Master Mix (Thermo Fisher, Waltham, MA) with 10 nM primers and then amplified by PCR (95°C for 10 min, 56°C for 30s, 95°C for 15s, 13 cycles).

Importantly, the multiplexed detection was achieved by PCR amplification with unique primer pairs (see Fig 1). For detection of total IgE, 1F and 1R primers were employed (shown in Fig 1 in dark blue and light blue); for total anti-OVA antibodies (of any isotype, including IgE), 2F and 2R primers were used (shown in Fig 1 in gold and yellow). For allergen specific IgE (IgE anti-OVA), 2F and 1R primers were used (shown in Fig 1 in gold and light blue). Each primer and PCR master mix were mixed with 25 µL of ligation solution in

separate wells. Then, the PCR reaction was diluted 1:20 in ddH2O and 8.5 µL of the diluted PCR samples were added to 10 µL 2x SYBR qPCR Master Mix (Life Technologies, Carlsbad, CA) with 1.5 µL primers (final concentration 690 nM). Again, total IgE was quantified by 1F and 1R primer pairs with qPCR (Bio-Rad CFX96 real-time PCR detection system). Total anti-allergen antibodies were quantified with qPCR by 2F and 2R primers. Specific IgE was quantified with 2F and 1R primers by qPCR. All analyses can be in different wells on the same qPCR plate for the same run.

To measure anti-peanut antibody responses in mice, a similar protocol was followed with few modifications. As probes, 1 fmol each of Ara-h1-2A, Ara-h1-2B, Ara-h2-3A, Ara-h2-3B, Ara-h3-4A, Ara-h3-4B, anti-IgE-1A and anti-IgE-1B were resuspended in 2 µL of Buffer C (2% BSA, 0.2% Triton X-100, 8 mM EDTA in PBS) and 15 µL of the solution was added to 15 µL 2x PCR Master Mix with 10 nM primers. The primer pairs used in PCR and qPCR reaction included 1F/1R, 2F/2R, 2F/1R, 3F/3R, 3F/1R, 4F/4R and 4F/1R. The overall process from sample input to assay completion was ~3-4 hours.

For the detection of anti-peanut antibodies in patients' plasma, we performed procedures similar to those mentioned above. For those data points with disagreement between the two methods (i.e., the values fell within the false positive (FP), false negative (FN) quadrants), it remains to be shown, e.g., based on analyses of larger cohorts of patients, which of the two methods will yield results that are more concordant with clinical assessments (e.g., clinical history, physical examination, and, importantly, the results of oral food challenges). We also assessed the limit of detection for CLIQ, following the National Committee for Clinical Laboratory Standards (NCCLS) EP17-A protocol 9, 10. Briefly, the limit of detection (LOD) is defined as the average of signals obtained with the blank specimen plus 3.29 standard deviations. Therefore, we calculated LODs of 0.95, 0.55 and 1.94 (ΔCt units) for anti-Ara h1, anti-Ara h2 and anti-Ara h3 sIgEs, respectively (indicated by the vertical red dashed-lines in Fig E9). As expected, the LODs are lower than the clinical cutoff values for each allergen-specific IgE.

Validation of ISAP with purified antibodies.

Dilution series of anti-ovalbumin IgE (AbD Serotec #MCA2259, Hercules, CA), IgE isotype control (Biolegend #401701, San Diego, CA) and anti-ovalbumin IgG (Abcam #ab17293, Cambridge, United Kingdom) were prepared by performing 10-fold serial dilution of each antibody stock solution into Buffer C solution (2% BSA, 0.2% Triton X-100, 8 mM EDTA in PBS). The number of

antibody molecules in each measurement was calculated by (1x10-6 L) x Antibody concentration (M). Therefore, the number of antibody in each dilution series ranged from 10-13 to 10-18 mol. Anti-IgE-1B and OVA-2A conjugates were used in these ISAP experiments. Primer 2F/1R were used for quantification. Data are shown in Fig 2A.

Validation of CLIQ with purified antibodies. Dilution series of anti-ovalbumin IgE, IgE isotype control and anti-ovalbumin IgG were prepared as described above. The number of antibody molecules also ranged from 10-13 to 10-18 mol. Anti-IgE-1A, Anti-IgE-1B, OVA-2A and OVA-2B were used in these CLIQ experiments. Primer pairs 1F/1R were used to quantify total IgE, primer pairs 2F/1R were used to quantify OVA-specific IgE, and primer pairs 2F/2R were used to quantify total anti-ovalbumin antibodies. Data are shown in Fig E2.

Data analysis.

All PCR assays were run alongside a Buffer C-only blank (2% BSA, 0.2% Triton X-100, 8 mM EDTA in PBS) to correct for run-to-run variations. The Ct value for each sample was determined by a single-threshold fluorescence value automatically chosen by the Bio-Rad software. For each sample, the PCR cycle number with a fluorescence value corresponding to the threshold value was defined as the cycle threshold (Ct) value. ΔCt is defined as the Ct value of the blank minus the Ct value of the samples. The value of ΔCt is proportional to the initial amplicon concentration in the PCR plate well. This amplicon concentration is then also proportional to the amount of target antibody. To determine the detection limit, a non-linear four-parameter logistic fit for an antibody dilution series is determined using XLSTAT (New York, NY). The limit of detection for a PCR-based assay is defined as the average ΔCt value of the buffer C-only blank plus 3.29 standard deviations of the blank 9, 10. Thus, the limit of detection value is calculated relative to the blank. A similar process was performed for dilution series of antibodies measured by ELISA to obtain the corresponding detection limit. For tests of specimens from mice undergoing OVA or peanut sensitization, we normalized the PCR-based signal to the signal observed at day 0.

Statistical analysis. For statistical analyses, unless otherwise specified, Mann-Whitney U tests were performed. We considered a P value of less than .05 to be statistically significant. Unless otherwise specified, data are shown as individual values or as mean ± S.E.M.

SUPPLEMENTARY MATERIALS

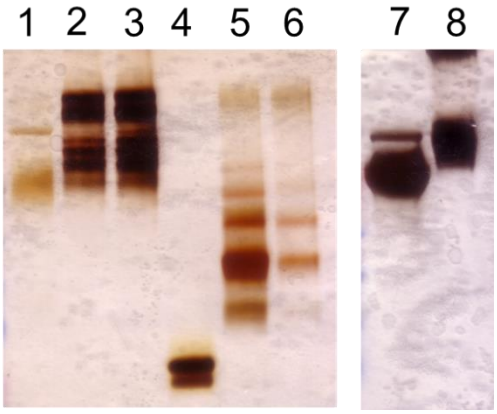

Figure E1. Representative silver stains of allergen-DNA and antibody-DNA conjugates. DNA conjugated allergens or antibodies have a higher mass than the unconjugated counterparts. Thus, one can use gel analysis together with silver staining to confirm the success of the conjugation protocols. Lane 1: unconjugated Ara-h1. Lanes 2 and 3: Ara-h1-DNA conjugates. Lane 4: unconjugated Ara-h2. Lanes 5 and 6: Ara-h2-DNA conjugates. Lane 7: unconjugated antibodies. Lane 8: conjugated antibodies. The multiple bands observed in Lane 2, 3, 5, 6 and 8 are due to different numbers of DNA molecules conjugated onto the proteins. For each protein, the median number of conjugated DNA molecules is 2.5-3.

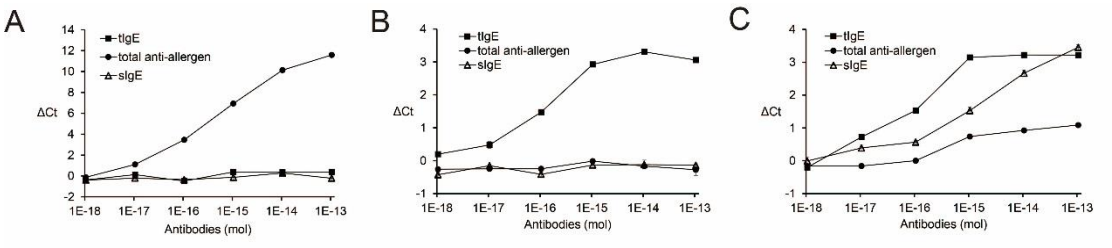

Figure E2. The integrated PCR-based Comprehensive Ligation-based Immunoglobulin Quantification (CLIQ) assay detects total IgE (tIgE) and allergen-specific (sIgE) with minimum cross-reactivity. We detected total IgE (tIgE, by proximity ligation assay, PLA), total anti-OVA specific immunoglobulins (total anti-OVA sIgs, by antibody detection by agglutination-PCR, ADAP) and anti-OVA specific IgE (anti-OVA sIgE, by isotype specific agglutination-PCR, ISAP) multiplexedly in a single assay (termed CLIQ, assay principles shown in Fig 1D). The specificity of the integrated CLIQ assay was assessed by testing separately dilution series of: (A) anti-OVA sIgG, (B) total IgE, and (C) anti-OVA sIgE, respectively. For instance, in Figure E2, A, the dilution series of anti-OVA sIgG was assayed by CLIQ. The PLA part of CLIQ measures total IgE and does not show signals (solid squares), the ADAP part of CLIQ, which measures total

anti-OVA immunoglobulins, yields a strong concentration-dependent signal (solid circles), and the ISAP part of CLIQ, which measures anti-OVA sIgE, yields no signals (open triangles). For many of the data points (mean ± S.E.M), the error bars were too small to be seen.

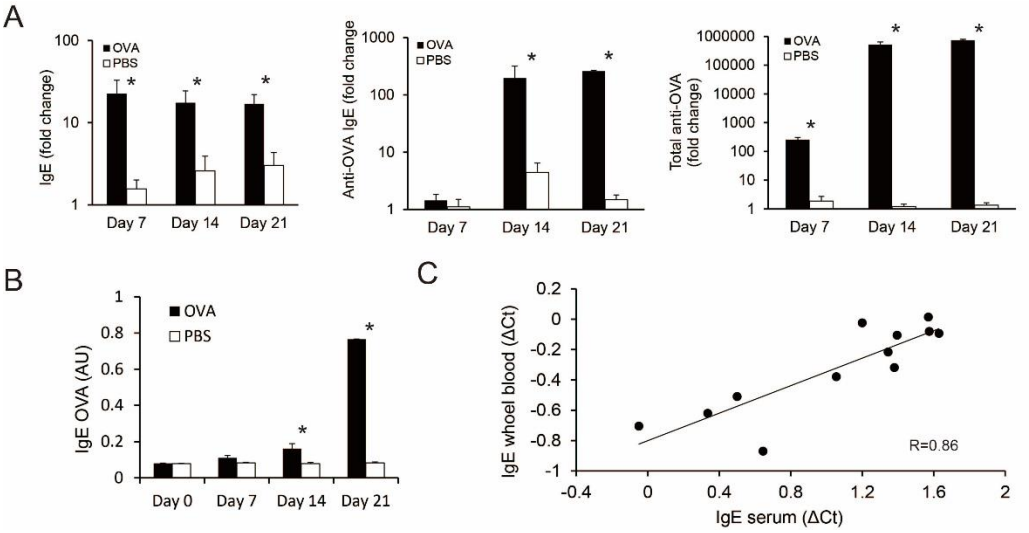

Figure E3. Integrated PCR-based CLIQ analysis of serum and blood from OVA-sensitized mice. Serum was collected from OVA-sensitized and PBS-mock-sensitized control mice on days 0, 7, 14 and 21. The PCR signal was normalized to the day 0 value for each mouse. (A) Enhanced levels of total IgE [tIgE] were detected starting on day 7, anti-OVA sIgE on day 14 and total anti-OVA immunoglobulins on day 7. (B) ELISA analysis of anti-OVA sIgE in the same set of serum samples. Enhanced levels of anti-OVA sIgE were first observed on day 14. (C) Correlation between results of PCR-based analysis of total IgE using serum and whole blood samples from the same mice. Serum and whole blood values displayed a correlation coefficient (R) of 0.86. (In A-C, * represents P < .05.)

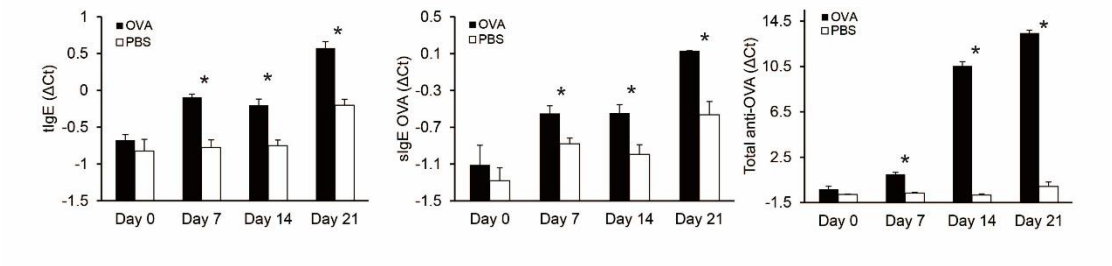

Figure E4. Integrated PCR-based CLIQ assay of whole blood of OVA-sensitized mice. In sensitized mice, PCR analysis of whole blood detected increased blood levels of total IgE [tIgE], anti-OVA sIgE, and total anti-OVA

immunoglobulins on day 7. (*P < .05).

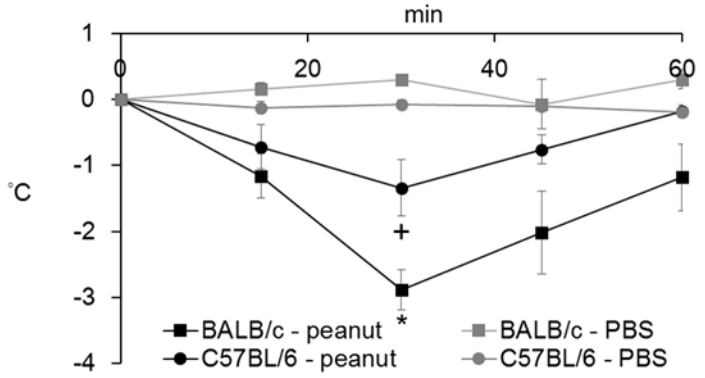

Figure E5. Body temperature after challenging peanut-sensitized mice with peanut extract or PBS. Peanut-sensitized BALB/c and C57BL/6 mice challenged with peanut exhibited a greater drop in body temperature than did identically-sensitized mice which were challenged with vehicle (PBS). (*P < .05 vs. values for the corresponding PBS-challenged BALB/c control mice, and + P < .05 vs. values for PBS-challenged C57BL/6 mice, by 2-WAY ANOVA).

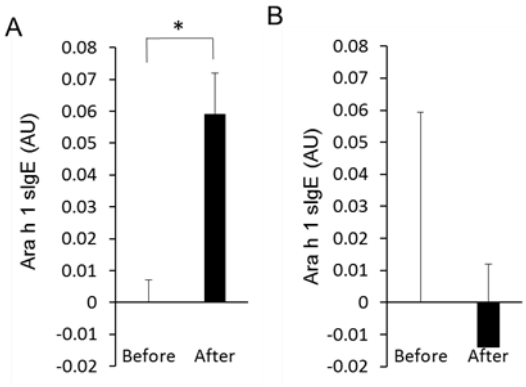

Figure E6. Ara h 1 sIgE ELISA analysis of mouse serum. The ELISA procedure is described in the Methods section (following the protocol of Smit, et al. 4[ref E2]). (A) Sera taken from mice before and after their oral sensitization to peanut (as described in Smit, et al.4 and Wijk, et al.5) were used as positive control specimens to validate the ELISA's ability to detect Ara h 1 sIgE. Briefly, 6 mg of peanut extract (#F171, Greer Laboratories, Lenoir, NC) with 15 µg of cholera toxin (List Biological Laboratories, Campbell, CA) per mouse were orally administered on days 0, 1, 2, 7, 14, 21, and 28. (n=3; five week-old female

C3H/HeOuJ mice [Jackson Laboratories, Bar Harbor, ME]). Serum was collected on day 0 (Before) and day 30 (After). A statistically significant difference in levels of Ara h 1 sIgE was observed before and after peanut sensitization (*P <0.05). (B) The sera shown in Figure 2D were re-analyzed by Ara h1 sIgE ELISA. No significant levels of Ara h 1 sIgE were detected.

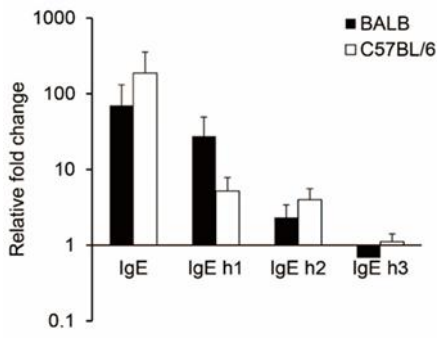

Figure E7. Fold change in levels of total and allergen-specific IgE between day 0 (before sensitization) and day 42 (after sensitization), as measured by integrated PCR-based CLIQ assay of serum obtained from peanut-sensitized BALB/c and C57BL/6 mice (n=5 mice per strain). None of the differences in the results for the two strains of mice were statistically significant. The h1, h2, h3 labels in the x-axis refer to Ara h1, Ara h2 and Ara h3, respectively.

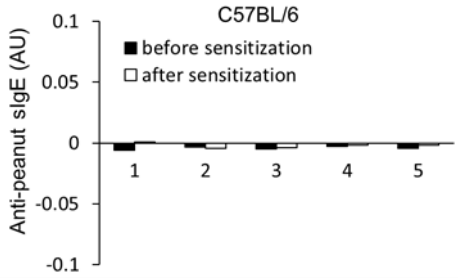

Figure E8. ELISA analysis of serum obtained from peanut-sensitized C57BL/6 mice (n=5 mice per strain) on day 0 (before sensitization) and day 42 (after sensitization). (These are the same serum samples analyzed by CLIQ assay in Fig E7.) No significant levels of anti-peanut specific IgE were detected.

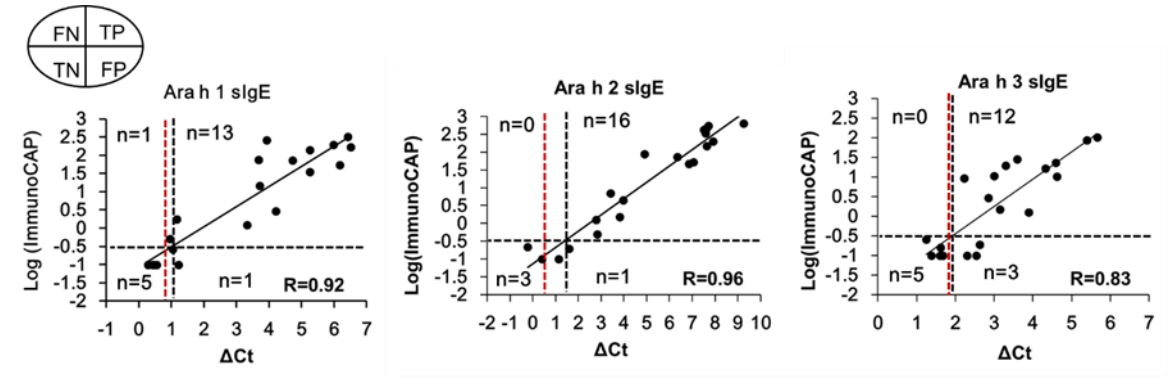

Figure E9. Comparison of results obtained by CLIQ versus ImmunoCAP. As described in Figure 2E, we plotted ISAP signals (ΔCt) in the X-axis and the logarithm of ImmunoCAP signals (kU/L) in the Y-axis (the PCR readout ΔCt is logarithmic by nature, therefore it was necessary to plot the logarithm of ImmunoCAP values for a valid comparison). In ImmunoCAP, 0.35 kU/L is the clinical cutoff for "sIgE positivity" (horizontal black dashed-lines). The CLIQ signals corresponding to 0.35 kU/L in ImmunoCAP are 1.11, 1.47, 1.99 (in ΔCt units) for anti-Ara h1, anti-Ara h2, and anti-Ara h3 sIgE, respectively (vertical black dashed-lines). Then, as shown in the oval cartoon divided into 4 sections, we divided the correlation graphs into four quadrants: true positive (TP), false positive (FP), false negative (FN) and true negative (TN). Most data points fell within the TP (n=13, 16 or 12, in the left to right panels) and TN (n=5, 3 or 5, in the left to right panels) quadrants, thus confirming the high level of concordance between the results of the two methods. The overall agreements were 90%, 95% and 85% for anti-Ara h1, anti-Ara h2 and anti-Ara h3 sIgE, respectively.

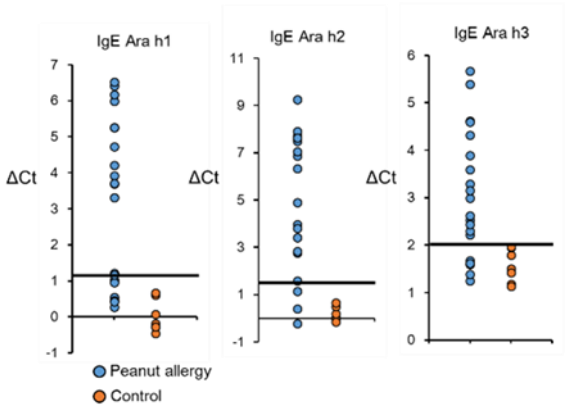

Figure E10. CLIQ assay clinical performance. To determine whether the assay cutoff established in Figure E9 is indeed clinically appropriate, we purchased 8 control serum samples of subjects not known to have peanut allergy from RDL Reference Laboratory (Los Angeles, CA). All samples were de-identified. We assayed these control serum samples with CLIQ. All control samples had sIgE

levels against Ara h 1, Ara h 2 and Ara h 3 below the cutoffs.

	Intra-assay	Inter-assay
Anti-Ara h 1 sIgE	10. 9%	3.9%
Anti-Ara h 2 sIgE	6.6%	7.1%
Anti-Ara h 3 sIgE	4.7%	3.9%

Figure E11. CLIQ assay reproducibility. We measured the same patient plasma specimens in 5 replicates in the same assay to determine the intra-assay variation, and also measured the same samples in 5 replicates on 4 different days to determine inter-assay variations. According to FDA guidance 11, the generally acceptable intra-assay and inter-assay variations for bioanalytical methods are 15%.

REFERENCES

1. Tuano KS, Davis, CM. Utility of component-resolved diagnostics in food allergy. Curr Allergy Asthma Rep. 2015;15:32.

2. Chapman MD, Wuenschmann S, King E, Pomés A. Technological innovations for high-throughput approaches to in vitro allergy diagnosis. Curr Allergy Asthma Rep. 2015;15:36.

3. Rahmatpour S, Khan AH, Nasiri Kalmarzi R, Rajabibazl M, Tavoosidana G, Motevaseli E, et al. Application of immuno-PCR assay for the detection of serum IgE specific to Bermuda allergen. Mol Cell Probes. 2016;S0890-8508:30078-0.

4. Johnston EB, Kamath SD, Lopata AL, Schaeffer PM. Tus-Ter-lock immuno-PCR assays for the sensitive detection of tropomyosin-specific IgE antibodies. Bioanalysis. 2014;6:465-76.

5. Fredriksson S, Dixon W, Ji H, Koong AC, Mindrinos M, Davis RW. Multiplexed protein detection by proximity ligation for cancer biomarker validation. Nat Methods. 2007;4:327-9.

6. Tsai CT, Robinson PV, Spencer CA, Bertozzi CR. Ultrasensitive Antibody Detection by Agglutination-PCR (ADAP). ACS Cent Sci. 2016;2:139-47.

7. Balbino B, Sibilano R, Starkl P, Marichal T, Gaudenzio N, Karasuyama H, et al. Pathways of immediate hypothermia and leukocyte infiltration in an adjuvant-free mouse model of anaphylaxis. J Allergy Clin Immunol. 2017;139:584-596.

8 Lansford R, Manis JP, Sonoda E, Rajewsky K, Alt FW. Ig heavy chain class switching in Rag-deficient mice. Int Immunol. 1998;10:325-32.

9. Mukai K, Gaudenzio N, Gupta S, Vivanco N, Bendall SC, Maecker HT, et al. Assessing basophil activation by using flow cytometry and mass cytometry in

blood stored 24 hours before analysis. J Allergy Clin Immunol. 2016;S0091-6749:30613-3.

Chapter 5
Concluding remarks

Chapter 5. Concluding remarks

In this thesis, I described the development of a series of nucleic acid based assays to quantify and detect antibodies. The first assay termed antibody detection by agglutination-PCR (ADAP) could be used to quantify antibodies of all classes (IgG, IgM, IgA, IgE and IgD), whereas the second assay dubbed isotype specific agglutination-PCR (ISAP) could be used to detect antibodies of a specific isotype. The two assays are complementary in that one would prefer one assay than the other under different circumstances. For instance, for autoimmunity such as type 1 diabetes (T1D), it appears that assays only detect IgG and assays that detect all isotypes do not perform differently in terms of clinical sensitivity and specificity. Hence, in T1D applications, one would prefer ADAP assay over ISAP. However, for other applications such as diagnosis of allergy, it is well known that only IgE based markers confer diagnostic value. Therefore, for allergy applications, one would use ISAP but not ADAP.

The use of ADAP and ISAP technology is likely to benefit researchers and clinicians by offering unprecedented sensitivity, high specificity, multiplex power and low sample consumption (1-2 μL). Critically, as opposed to other high performing immunoassays, ADAP and ISAP use low cost reagents and readily available instruments as readout (real-time quantitative PCR).

In the near future, I wish to continue the development of ADAP and ISAP by porting the methodology to automation system such that as little human interventions are required. Such efforts should lead to a high quality immunoassays that can be deployed in wide range of research and clinical settings.